IEEE Access
Multidisciplinary ⋮ Rapid Review ⋮ Open Access Journal

Received September 27, 2020, accepted October 24, 2020, date of publication November 3, 2020,
date of current version November 16, 2020.

Digital Object Identifier 10.1109/ACCESS.2020.3035447

Towards Energy Efficient Load Balancing for Sustainable Green Wireless Networks Under Optimal Power Supply

MD. SANWAR HOSSAIN[1], (Graduate Student Member, IEEE), ABU JAHID[2], (Graduate Student Member, IEEE), KHONDOKER ZIAUL ISLAM[3], MOHAMMED H. ALSHARIF[4], KHONDOKAR MIZANUR RAHMAN[5], MD. FAYZUR RAHMAN[6], AND MD. FARHAD HOSSAIN[7], (Member, IEEE)

[1]Department of Electrical, Electronics and Communication Engineering, Military Institute of Science and Technology, Dhaka 1216, Bangladesh
[2]Electrical and Computer Engineering, University of Ottawa, Ottawa, ON K1N 6N5, Canada
[3]Department of Electrical and Electronic Engineering, Bangladesh University of Business and Technology, Dhaka 1216, Bangladesh
[4]Department of Electrical Engineering, College of Electronics and Information Engineering, Sejong University, Seoul 05006, South Korea
[5]School of Engineering and the Built Environment, Birmingham City University, Millennium Point, Birmingham B4 7XG, U.K.
[6]Department of Electrical and Electronic Engineering, Green University of Bangladesh, Dhaka 1205, Bangladesh
[7]Department of Electrical and Electronic Engineering, Bangladesh University of Engineering and Technology, Dhaka 1205, Bangladesh

Corresponding authors: Md. Sanwar Hossain (sanwareee@gmail.com) and Mohammed H. Alsharif (malsharif@sejong.ac.kr)

ABSTRACT The enormous growth in the cellular networks and ubiquitous wireless services has incurred momentous energy consumption, greenhouse gas (GHG) emissions and thereby, imposed a great challenge to the development of energy-efficient sustainable cellular networks. With the augmentation of harvesting renewable energy, cellular base stations (BSs) are progressively being powered by renewable energy sources (RES) to reduce the energy crisis, carbon contents, and its dependency on conventional grid supply. Thus, the combined utilization of renewable energy sources with the electrical grid system is proving to be a more realistic option for developing an energy-efficient as well as an eco-sustainable system in the context of green mobile communications. The ultimate objective of this work is to develop a traffic-aware grid-connected solar photovoltaic (PV) optimal power supply system endeavoring the remote radio head (RRH) enabled heterogeneous networks (HetNets) aiming to minimize grid energy consumption and carbon footprint while ensuring long-term energy sustainability and energy efficiency (EE). Moreover, the load balancing technique is implemented among collocated BSs for better resource blocks (RBs) utilization and thereafter, the performance of the system is compared with an existing cell zooming enabled cellular architecture for benchmarking. Besides, the techno-economic feasibility of the envisaged system has been extensively analyzed using HOMER optimization software considering the dynamic nature of solar generation profile and traffic arrival rate. Furthermore, a thorough investigation is conducted with the help of Monte-Carlo simulations to assess the wireless network performance in terms of throughput, spectral efficiency (SE), and energy efficiency as well under a wide range of design scenarios. The numerical outcomes demonstrate that the proposed grid-tied solar PV/battery system can achieve a significant reduction of grid power consumption yielding up to 54.8% and ensure prominent energy sustainability with the effective modeling of renewable energy harvesting.

INDEX TERMS Load balancing, cell zooming, green communication, energy-efficiency, eco-friendly, sustainability.

I. INTRODUCTION

Over the last decade, the high-tech advancement in mobile devices together with the increasing popularity of intensive multimedia applications has accelerated the astounding rise of data demand. A recent study on global mobile data traffic forecasted that the unique mobile subscriber's number would increase to 6.2 billion by the end of 2023 [1]. To satisfy the higher demand of users, telecom operators are increasingly deploying more BSs and hence, leading to an increase in a vital portion of the energy utilization in mobile communication. The international energy agency (IEA) in its

The associate editor coordinating the review of this manuscript and approving it for publication was Cunhua Pan.

latest global energy projection, the World Energy Outlook 2018 (WEO2018), has reported that global energy demand is expected to grow by about 27%, or 3,743 million tons oil equivalent worldwide from 2017 to 2040 [2]. Authors in [3] mentioned that the annual energy consumption by the mobile industry has increased from 219 TWh in 2007 to 519 TWh in 2019, and it is speculated that the demand rises at a yearly rate of 10%. Consequently, the electricity bill of telecom networks globally amounts to above ten billion per year. It is expected that the GHG outflow emitted by the information and communication technology (ICT) sector will increase from 1700 quintals in 2014 to 235 quintals by 2020, with 51% of CO_2 emissions generated from the telecom industry [4], [5].

Another downside, BSs in the radio access networks (RAN) contribute almost 60-80% of entire energy expenditure and place a heavy burden on the electrical grid (EG) supply to deal with the question of sustainable power issue [6], [7]. In response to the request for reducing grid energy consumption and environmental aspects, cellular operators are widely focusing on green communications concentrating on the environmental implications. Recently, access networks in green radio communication systems supplied by sustainable and reliable renewable energy have brought a remarkable result, which has drawn great attention in both industry and academia [8]–[11]. For instance, Huawei [10] designed a green BSs under 3G network in Bangladesh powered by solar PV to reduce the sole dependency on the electric grid.

It is commonly believed that an electrical grid system is enough as a power source for BS where the grid connection exists. The use of grid energy emits harmful carbon contents which significantly causes air pollution, the rise of world temperature, and damage of the ozone layer. Furthermore, the lower efficiency and routine operation and maintenance make the system much less reliable and resulting in outage during grid failure. Being motivated by the aforementioned issues, the utilization of RES such as solar PV at the BS site providing operators the option to develop green access cellular networks through the deduction of harmful greenhouse gas discharge. Numerous studies [12]–[15] have been carried out for curbing down the energy costs by adopting renewable energy sources to power large-scale cellular network. Still, research in this field is not saturated. Most of the authors have not analyzed the cost-effective solution for long term evolution (LTE) cellular networks with real traffic patterns.

Nowadays, modern cellular systems are required to manage the excessive number of linked equipment (millions per macrocell), excessive bit rate (tens of Gbps), improved spectral efficiency, enhanced energy efficiency, strong reliability (∼99.999%), intensely low latency (∼1 ms) for data-intensive, mission-critical and time-critical applications [16], [17]. Consequently, investigations for finding ways to develop a more competent cellular network have been carried out in recent times [18]. Typically conventional macrocell architectures are designed to cater to larger spectral areas that may often fail to attain the desired throughput to support seamless broadband service to uplink users. Besides, users move far away from the macro BS and often cause severe inter-cell interference. The weak indoor penetration and the appearance of dead spots considerably reduce the indoor coverage under the traditional macrocell scenario. As a potential solution to overcome these issues, heterogeneous networks (overlay of small cell networks like micro/pico/femto cells with macro BS) offer significant network performance leap by means of higher network capacity and better coverage [19]–[23]. HetNets are the multi-tier cellular network, where the macro BSs act as a mother BS and provide a uniform coverage area. On the other hand, the micro and pico/femto cells act as supporting BSs which consume low energy due to the smaller amount of coverage area. Hence, the installation of HetNets potentially improve spatial reuse, and the capacity in the hotspot can minimize the coverage hole of the cellular network in dead spots which can save a significant amount of energy as well as extend the coverage while ensuring seamless connectivity and mobility in future generation cellular systems [24].

In this trend, load balancing has appealed much consideration as a talented way out for higher resource allocation, better system enactment, and reduced operational expenditure as well. Load balancing is an efficient technique for adjusting the load and relieving the congestion among heterogeneous networks in the upcoming 5G networks. With the introduction of load balancing techniques, a cellular network can gain in different ways, such as the effective exercise of frequency bands, improvement in coverage for cell-edge users, and boosting in overall network throughput [25], [26]. However, the concept of load balancing can be applied for improving the spectral efficiency of mobile access set-ups. On the other hand, the load balancing mechanism flexibly adjusts BS coverage depending on experienced traffic density and enhances the service quality of an entire cellular network through balancing the traffic among surrounded BSs in a cluster. Authors in [27] proposed a distributed user association based load balancing algorithm to balance the load among the neighboring BSs. Reference [28] introduces an empirical load balancing algorithm that can be used to optimize the range of the HetNets. Therefore, the load balancing techniques are used for redistributing the load among the active BSs and can benefit in many ways, such as efficient utilization of frequency bands, enhancement in coverage for cell-edge users, and increment in overall network throughput. In this paper, the concept of load balancing is employed for improving the energy efficiency performance under optimal power supply scenarios. Throughput aware load balancing based on the effective data rate of users [29] and energy-aware resource management [30] under hybrid power supplies is comprehensively analyzed focusing on minimum grid power consumption. Instead of the conventional throughput maximization technique, authors [31] proposed a joint user association and power control algorithm for load balancing in modern telecom networks. On the other hand,

a cluster-based load balancing policy is adopted to maximize the network throughput (achieved 6.42% better performance compared to the non-load balancing technique) in reference [32].

In a cellular network, the non-uniform traffic density due to the tempo-spatial variations of mobile subscribers has incurred an unnecessary use of energy [32]–[34]. To overcome this problem, telecom operators are dedicated to developing green mobile communication, which adaptively adjusts the cell size according to the user profile. This condition is supported by a conceptual strategy called ''cell zooming'' to optimize the energy consumption of base stations according to the user condition. In summary, cell zooming is the increment or decrement of cell size from its originally designed size under the traffic condition of the cell. This reduces the traffic load in its neighboring cells and some cells can even go switch-off, which will result in energy saving. Recently, various techniques have been proposed by turning off the BSs to minimize the energy consumption of the cellular network [35]–[37]. For saving energy, LTE proposes switching off the evolved node base station (eNBs) at low-traffic times [38]. Reference [37], proposed a cell zooming concept to minimize energy consumption by integrating BS switching. Authors in [39], [40] proposed a multipoint coordinated cell zooming concept, where the actual size of the cell does not change but the cell size is virtually extended. It is commonly known as virtual cell zooming or virtual MIMO system. A relay assisted cell zooming concept is presented in [40], [41], where a moveable or fixed relay station is placed at the edge of the original cell to extend the coverage area. References [42], [43] introduced a physically adjustable cell zooming technique, where the cell size is adjusted by changing the different parameters such as antenna height, antenna tilt, transmitted power, etc. Energy efficiency and spectrum aware cell zooming are conducted to tackle the upsurge in traffic load in [44], [45]. The wireless network performance enhancement contemplating adaptive cell zooming and sleeping mode mechanism for ultra-dense HetNet with green power supply is pointed out in [46], [47]. Reference [48] proposed a data-driven energy minimization problem implementing a cell zooming algorithm leveraging the tradeoff between blockage ratio and energy saving issue. Reference [49], introduces a theoretical optimization method for saving energy by switching off the BSs. Implementation of the cell zooming concept for the heterogeneous network is presented in [37] without taking into account actual traffic arrival rate and average energy savings for green cellular infrastructure. However, some of the schemes are failed to capture the load-dependent power utilization in BSs resulting in overestimations. Moreover, many of them presented either very basic algorithms ignoring the actual locations of users, or no algorithm at all.

The prime concern of this work is to develop a traffic-aware energy-efficient and sustainable cellular network that inherently minimizes the pressure on the public utility grid and reduces the carbon contents. The optimization of renewable energy utilization is done using a HOMER software taking into account different types of constraints. Moreover, Matlab based Monte-Carlo simulations are carried out for measuring the performance metrics of the wireless network under a wide range of system scenarios. The key contributions of this work can be summarized as follows:

- To propose a grid-tied solar PV/battery system for powering the LTE macro/micro-cellular base stations with guaranteed continuity of services. Notably, the solar PV panels play as a primary supply whereas the electrical grid system supplies energy as a secondary source for operating BSs during the shortage or absence of solar PV system. Moreover, the battery bank ensures guaranteed continuity of supply by supplying the backup power.
- To examine the effectiveness of the proposed system in terms of optimal system architecture, techno-economic criteria, and carbon footprints considering the intermittent behavior of solar intensity and traffic rate. In addition, the impact of BS transmits power, and different LTE system bandwidth on the performance metrics are critically illustrated.
- To evaluate the throughput, energy efficiency, and spectral efficiency performance of the wireless network taking into account the inter-cell-interference and wireless channel model including shadow fading.
- A load balancing technique is developed for maximizing the SE and EE as well through optimal utilization of green energy, while the entire system is still envisioned by hybrid power sources as outlined above. After that, a heuristic algorithm for load balancing mechanism and resource block allocation technique is proposed.

The rest of the manuscript is outlined as follows: Section II contains the system architecture and modeling of the proposed system. Section III illustrates the cost modeling and optimization formula. Section IV demonstrates the performance analysis with insightful comments. Section V represents the conclusions of the manuscript highlighting the key outcomes.

II. SYSTEM ARCHITECTURE AND MODELING

The schematic diagram of the solar PV/EG/battery-powered cellular network system is shown in Fig. 1. An LTE macro BS usually consists of transceivers (TRXs), power amplifiers (PAs), a radio-frequency (RF) unit, a baseband (BB) unit, a DC-DC power supply, and a cooling system [50], [52], [53]. The BS is powered by solar PV plus public utility grid and backup power is provided by the battery bank. BS consumes energy from the electrical grid system in case of the deficiency of solar-generated power. We consider three different BS configurations namely macro 2/2/2, macro omni, and micro. Modern macro cellular BSs have widely adopted the concept of a distributed base station in which the baseband signal processing unit is separated from the radio-frequency unit that is defined as a remote radio head.

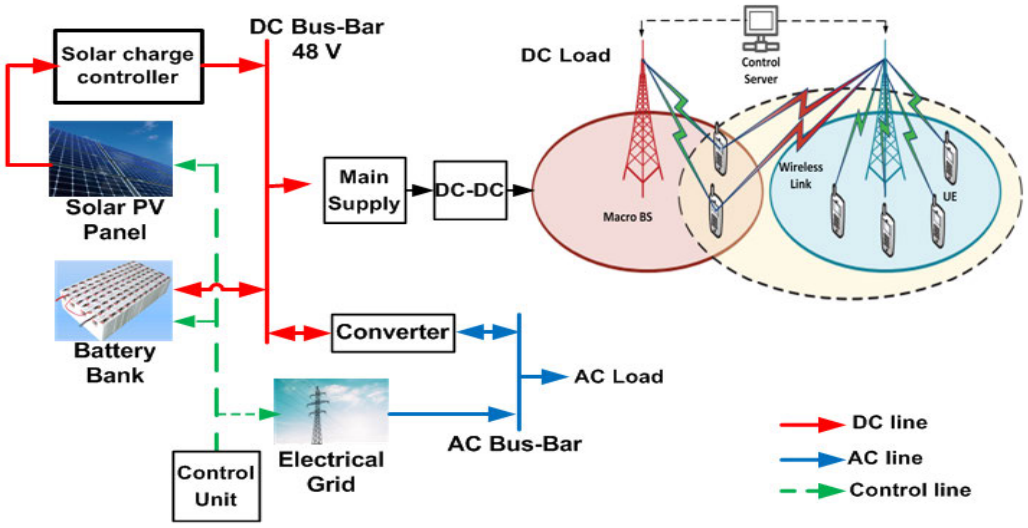

FIGURE 1. Schematic diagram of the proposed system.

A. SOLAR PV PANEL

Solar PV panels are arrays consist of series/parallel connected multiple solar cells to transform sunlight into electricity. The amount of solar energy generated by the solar PV panel is mostly affected by the location, materials/ tilt of the solar panels, and energy harvesting technology. Moreover, the internet of things (IoT) based smart monitoring system can be incorporated to control the generated power of the solar PV system [51]. The annual energy produced by the solar PV panel can be determined as follows [52]

$$E_{PV} = R_{PV} \times PSH \times \eta_{PV} \tag{1}$$

where R_{PV} expresses rated capacity for solar PV panel (kW), PSH means peak solar hour calculated from the average value, and η_{PV} is the panel efficiency. The monthly statistic of solar radiation and the clearness index are presented in Fig. 2.

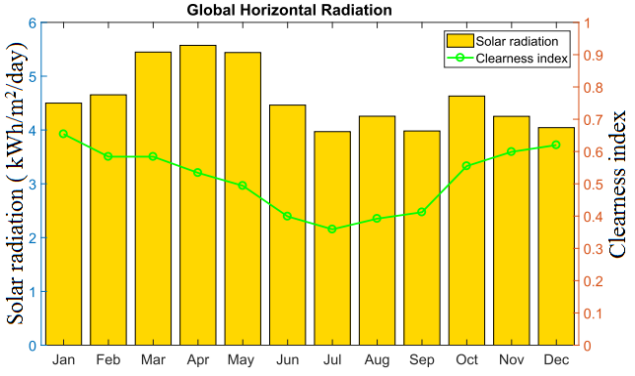

FIGURE 2. The monthly statistic of solar radiation and the clearness index.

B. ELECTRICAL GRID

Generally, the electrical grid is an interconnected system that is used for supplying power to the load. In this work, the proposed solar PV/battery system has been connected to the utility grid for sharing the excess electricity to or from the grid, which ensures the maximum utilization of renewable energy by maintaining the quality of services (QoS).

C. BATTERY BANK

A battery bank is an auxiliary device which stores surplus electricity during the peak generation and supplies the BS in case of energy shortage or outage. The battery state of charge (B_{SOC}) is an important factor in selecting storage devices. The minimum state of charge is the minimum discharge limit of the battery. The depth of discharge (B_{DOD}) implies the maximum energy supply limit from the battery bank determined from the equation below [52]

$$B_{DOD} = (1 - \frac{B_{SOC_{min}}}{100}) \tag{2}$$

However, the autonomy of the battery system (B_{aut}) indicates the probable period limit up to that the storage device can supply the essential electricity to run BS load if the solar PV array is in failure. The battery bank autonomy can be represented as follows [52]

$$B_{aut} = \frac{N_{batt} \times V_{nom} \times Q_{nom} \times B_{DOD} \times (24h/day)}{L_{BS}} \tag{3}$$

where N_{batt} is the total battery number used in the battery bank, V_{nom} is the theoretical voltage value of a single battery (V), Q_{nom} is the nominal capacity of a single battery (Ah) and L_{BS} is the average daily BS load in kWh.

The lifecycle of the battery (L_{batt}) is directly related to the replacement costs of the proposed project can be calculated using (4) [52]

$$L_{batt} = min(\frac{N_{batt} \times T_{batt}}{T_a}, R_{batt,f}) \tag{4}$$

where T_{batt} is the lifetime of a single battery (kWh), T_a is the annual battery throughput (kWh/year) and $R_{batt,f}$ is the battery float life (year).

TABLE 1. BS power consumption at maximum load under 10 MHz bandwidth [54].

Components	Parameters	Macro 2/2/2	Macro Omni	Micro
	P_{TX} [W]	20	20	6.3
	Feeder loss σ_{feed} [dB]	3	0	0
PA	Back-off [dB]	8	8	8
	Max PA out [dBm]	54	51	46
	PA efficiency η_{PA} [%]	31.1	31.1	22.8
	Total PA, P_{PA} [W]	128.2	64.4	27.7
RF	P_{TX} [W]	6.8	6.8	3.4
	P_{RX} [W]	6.1	6.1	3.1
	Total RF, P_{RF} [W]	12.9	12.9	6.5
BB	Radio (inner Tx/Rx) [W]	10.8	10.8	9.1
	Turbo code (outer Tx/Rx)	8.8	8.8	8.1
	Processors [W]	10	10	10
	Total BB, P_{BB} [W]	29.6	29.6	27.3
DC-DC	σ_{DC} [%]	7.5	7.5	7.5
Cooling	σ_{cool} [%]	10	0	0
Main Supply	σ_{MS} [%]	9	9	9
Sectors		3	1	1
Antennas		2	1	2
Total [W]		**754.8**	**125.8**	**144.6**

D. CONVERTER

Among the different types of converters, an inverter is an instrument which is used to convert the AC voltage into DC voltage. The capacity of the inverter mostly depends on the size of the load and inverter efficiency and can be calculated as follows [52]

$$C_{inv} = (\frac{L_{AC}}{\eta_{inv}}) \times \sigma_{sf} \tag{5}$$

where L_{AC} represents the peak AC load in kW, is the efficiency of the inverter in %, and σ_{sf} is the safety factor.

E. BS POWER CONSUMPTION MODEL

Modeling and optimal sizing of the proposed system are directly related to BS energy consumption. Table 1 summarizes the power consumption of every single component of the LTE macro/micro BS for the highest traffic intensity. On the other hand, Table 2 represents the BS key parameters. In a practical cellular network, the incoming traffic arrival rate is time-varying and the BS energy demand is traffic sensitive. An approximate traffic pattern can be predicted by utilizing the Poisson distribution model as follows [55]

$$\lambda(t) = \frac{p(t,\alpha)}{max[p(t,\alpha)]} \tag{6}$$

$$p(t,\alpha) = \frac{\alpha^t}{t!}e^{-\alpha} \tag{7}$$

where $\lambda(t)$ is the normalized traffic distribution, $p(t,\alpha)$ is the Poisson distribution function of traffic demand at a particular point of time, and α is the mean value.

The total power utilization of a BS as a function of traffic intensity (χ) can be represented as follows [55]

$$P_{in} = \begin{cases} N_{TRX}(P_1 + \Delta_p P_{TX}(\chi - 1)), & \text{if } 0 < \chi \leq 1 \\ N_{TRX}P_{sleep}, & \text{if } \chi = 0 \end{cases} \tag{8}$$

TABLE 2. BS key parameters [22].

BS Type	N_{TRX}	P_{TX} [W]	P_0 [W]	Δ_p	P_{Sleep} [W]
Macro 2/2/2	6	20	84	2.8	56
Macro Omni	1	20	84	2.8	56
Micro	2	6.3	56	2.6	39

where $P_1 = P_0 + \Delta_p P_{TX}$ is the maximum power consumption of a BS sector, N_{TRX} is the total number of the transceiver, Δ_p is the load dependency power gradient and is the consumption at idle state.

The maximum power consumption of the base station as a function of different types of losses is determined as follows [55]

$$P_1 = \frac{P_{BB} + P_{RF} + P_{PA}}{(1-\sigma_{DC})(1-\sigma_{MS})(1-\sigma_{cool})} \tag{9}$$

$$P_1 = \frac{N_{TRX}\frac{BW}{10MHz}(P'_{BB} + P'_{RF}) + \frac{P_{TX}}{\eta_{PA}(1-\sigma_{feed})}}{(1-\sigma_{DC})(1-\sigma_{MS})(1-\sigma_{cool})} \tag{10}$$

where σ_{DC}, σ_{MS}, and σ_{cool} respectively represent the loss associate with the DC-DC regulator, main supply, and cooling system. N_{TRX} is the total number of antennas in a base station and is the maximum transmission power in W. The P'_{BB} and P'_{RF} are the baseband and RF power consumption respectively for the given 10 MHz transmission bandwidth.

The total BS energy consumption according to (8) is listed in Table 3. The amount of power drawn by the different BSs configurations is shown in Fig. 3. Fig. 4 demonstrates the daily traffic load profile which has been calculated using (8).

TABLE 3. BS annual energy consumption in kWh.

BS Type	Annual consumption (kWh)
Macro 2/2/2	5,042
Macro Omni	854
Micro	1,117

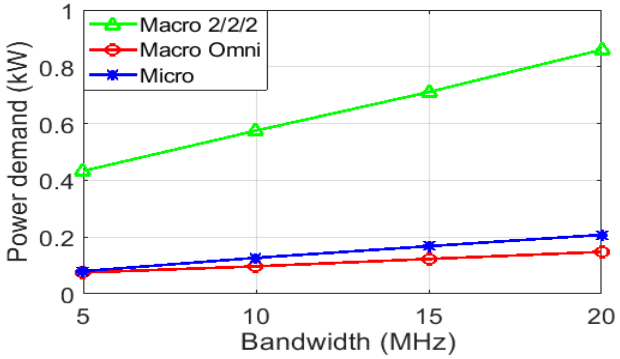

FIGURE 3. Power demand for the different types of BS.

F. PERFORMANCE METRICS

In this work, the throughput, energy efficiency, and spectral efficiency performance of the two-tier LTE cellular network are critically evaluated taking into account the tempo-spatial

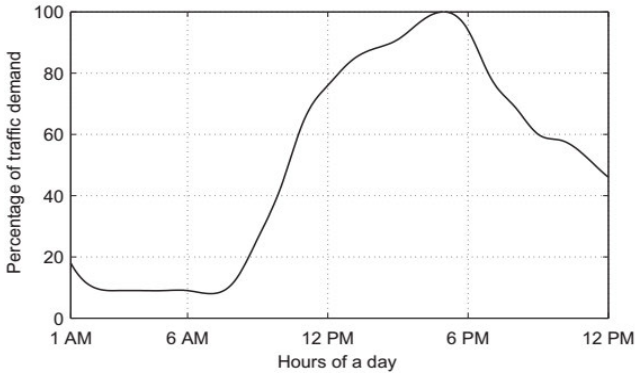

FIGURE 4. Dynamic traffic profile of the Dhaka city.

variation of traffic intensity. According to Shanon's information capacity theorem, total reachable throughput (in kbps) of the cellular network can be estimated by the following equation [57]

$$C_{total}(t) = \sum_{k=1}^{U} \sum_{i=1}^{N} \Delta log_2(1 + SINR_{i,k}) \tag{11}$$

where $SINR_{i,k}$ is the received signal-to-interference-plus-noise-ratio at k^{th} UE located in BS B_i. N is the number of transmitting BSs and U is the total number of UEs in the network.

The energy efficiency of the wireless network is one of the vital factors for assessing performance. The term ''energy efficiency'' denotes the number of bits transmitted per joule of energy. The performance metrics energy efficiency is denoted as η_{EE} and can be expressed as follows [57]

$$\eta_{EE} = \frac{C_{total}}{P_{net}} \tag{12}$$

where P_{net} is the total power consumed in all the BSs at time t and can be calculated by using (8). The spectral efficiency (SE) is represented in bps/Hz and can be determined by the following formula [25]

$$\psi_{i,k} = \begin{cases} 0 & if\ SINR_{i,k} < SINR_{min} \\ \xi log_2(1 + SINR_{i,k}) & if\ SINR_{min} \leq SINR_{i,k} < SINR_{max} \\ \psi_{max} & if\ SINR_{i,k} \geq SINR_{max} \end{cases} \tag{13}$$

where $0 \leq \xi \leq 1$, $SINR_{min}$, ψ_{max} and $SINR_{max}$ are the attenuation factors accounting the implementation loss, minimum SINR, maximum SE, and the SINR at which ψ_{max} is achieved. Then the number of required RBs for UE k of class j can be estimated by [25]

$$\beta_{i,k}^{(j)} = \frac{R_{i,k}^{(j)}}{W_{RB}\psi_{i,k}} \tag{14}$$

where $R_{i,k}^{j}$ is the required data rate in bps, and W_{RB} is the bandwidth per RB in Hz (e.g., 180 kHz in LTE).

The number of total resource block (n_{RB}) that is required for the desired system bandwidth can be calculated as follows

$$n_{RB} = \frac{BW}{W_{RB}} \tag{15}$$

Hence, the total number of simultaneous users (N_{SU}) connected to the network can be determined as follows

$$N_{SU} = \frac{n_{RB}}{R_{i,k}^{(j)}} \tag{16}$$

The throughput, energy efficiency, and spectral efficiency metrics of the wireless network are determined using the Monte-Carlo based Matlab simulation. The simulations are accomplished by averaging around 10,000 iterations bearing in mind the time-varying traffic density. It is also considered that every user is associated with at least one resource block (RB). The technical parameters and their values for the basic parameters of the Monte-Carlo simulation setup are summarized in Table 4.

TABLE 4. Technical parameters and their value for the Matlab simulation setup [57].

Parameters	Value
Resource block (RB) bandwidth	180 kHz
System bandwidth, BW	5,10,15,20 MHz
Carrier frequency, f_c	2 GHz
Duplex mode	FFD
Cell radius	1000 m
BS Transmission power	43 dBm
Noise power density	-174 dBm/Hz
Number of sectors	3
Number of antennas	2
Reference distance, d_0	100 m
Path loss exponent, α	3.574
Shadow fading, X_σ	8 dB
Access technique, DL	OFDMA
Traffic model	Randomly distributed

To minimize the number of active BSs without sacrificing QoS can be attained through demand shifting from lightly loaded BSs to the surrounded BSs. Based on the statistical data, the BSs experiencing low traffic arrivals transfer its load to neighboring BS and thereby enter into sleep mode. It is to be noted that the surrounded BSs are handling the new arrivals in such a way that it would not lose their performance by means of data transmission services and also reserve 5% backup resource blocks in order to ensure robust QoS during peak periods. The key difference from the cell zooming concept is that it does not need to depend on the input power supplies over the zooming hours. Owing to the stochastic nature of RE production, wireless network performance might have conflicts. In this paper, we first designed the dimension of optimal power supply capacity and then measured the additional load carrying capability implementing the load-balancing technique.

G. CELL ZOOMING CONCEPT

The traffic density of a cellular network varies over time and space due to the mobility of the user and the dynamic

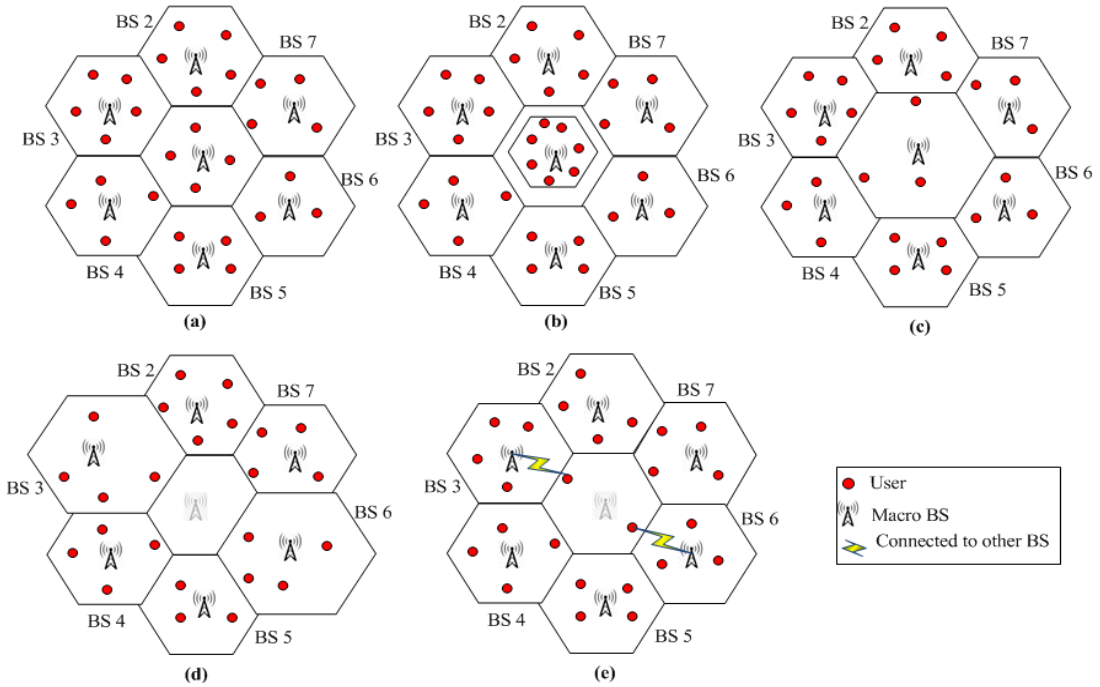

FIGURE 5. Operational mode of cell zooming (a) Cells without zooming, (b) Central cell zoom in during higher traffic density, (c) Central cell zoom out during lower traffic density, (d) Central cell in sleep mode and neighboring cells zoom out, (e) Central cell in sleep mode and neighboring cells operate cooperatively.

nature of many data applications. For instance, the traffic density in the office areas is higher and lower in the domestic areas during the daytime. This event is going to reverse in the evening. As a result, there exists always some higher density BSs and some lower density BSs in a cluster. In this case, the load balancing and cell zooming techniques can be applied to adjust the load, which will significantly increase the energy efficiency ensuring the service quality of the user equipment.

In this subsection, the basic concept of the traffic-aware load balancing and cell zooming is illustrated, which has the potential to handover the peak traffic demand among the neighboring base stations to attain a greater level of system performance. The fundamental concept of traffic steering based cell zooming technique is presented in Fig. 5. In this work, we consider a two-tier LTE cellular network with a hexagonal layout formed by 19 BSs. Where one BS is placed at the center of the hexagonal and the other eighteen BSs are deployed encompassed the center cell as shown in Fig. 5(a). All the BSs are connected to the control server for coordination. According to the traffic loads, received signal power, and energy availability of the BSs, the control server decides to zoom in, zoom out, and sleep mode of the cells. For making simple, the cell zooming principle is presented for seven BSs as shown in Fig. 5.

If the traffic intensity of the central BS is higher than the predefined value, the control server provides information to reduce the cell size by zooming in as shown in Fig. 5(b). On the other hand, if the mobile users (MUs) move out from the central BS and make the neighboring BS congested, the control server broadcasts the necessary information to zoom out the cell to avoid overflow of the neighboring BS as shown in Fig. 5(c). Moreover, if the traffic intensity of the central BS is very low and the collocated BSs has the capability to take all the MUs, then the low-density center BS will go to sleep mode to reduce the energy consumption as shown in Fig. 5(d). In this case, the neighboring BSs can be zoom out if they are in low density otherwise serve the left MUs by transmitting cooperatively as in Fig. 5(e). However, the sleep mode provision is suitable for the low traffic density areas during the off-peak hours. The amount of load received by the low traffic density cell depends on their unused resource blocks and renewable energy availability. For better understanding, the cell zooming algorithm is presented in a flowchart form as shown in Fig. 6.

In the cell zooming technique, the channel condition and user requirements in the network are collected by the control server, while resource allocation and cell zooming operations are performed in a centralized way. The details of the resource allocation is as follows:

1) RESOURCE ALLOCATION

A resource block (RB)is the lowest unit of physical resources that are assigned to every user. In the time domain, the resource block is one slot long. In the frequency domain, the resource block is 180 kHz wide and either 12 $\times$ 15 kHz subcarriers or 24 $\times$ 7.5 kHz subcarriers wide. For most of the channels, the number of subcarriers associated per RB is 12. As an example, a 5 MHz downlink signal can be expressed as 25 resource blocks wide or 301 subcarriers wide (DC

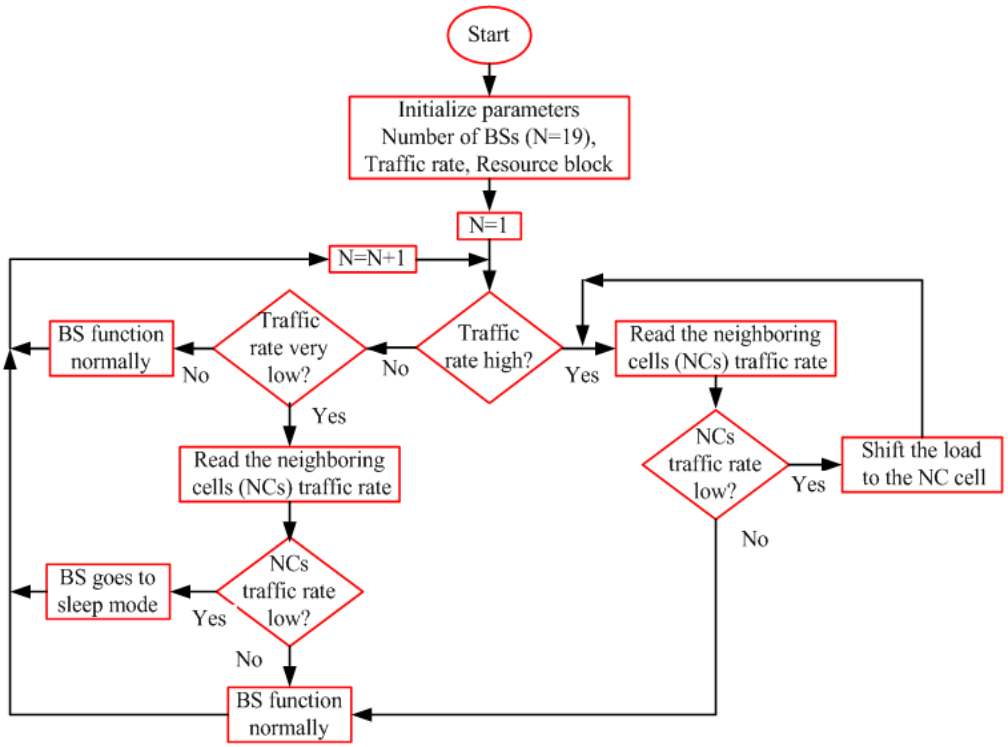

FIGURE 6. Flow chart of the traffic guided load balancing.

subcarrier is not involved in an RB). In the LTE network, 10% of the available bandwidth is used as a guard band for avoiding overlapping [58]. The standard bandwidth and corresponding resource block and subcarriers for both uplink and downlink conditions are presented in Table 5.

TABLE 5. Frequency measurement.

Bandwidth	Resource Blocks	Subcarriers (downlink)	Subcarriers (uplink)
1.4 MHz	6	73	72
3 MHz	15	181	180
5 MHz	25	301	300
10 MHz	50	601	600
15 MHz	75	901	900
20 MHz	100	1206	1200

The number of resource blocks allocated for the individual BS is determined based on the operating bandwidth. The individual BS use their allocated RBs according to the user requirement. In every time slot, this decision has been taken by the allocation algorithm. If one RB cannot fulfill the target requirement of a UE throughput then another RB is allocated according to the availability of free RBs. So, the total bandwidth allocated for a single user can be calculated from the multiplication of total RB allocated for the user and the BW of a single RB. The detailed procedure of the resource block algorithm is presented in Table 6.

In the resource block algorithm, $k = UE_1, UE_2, \ldots UE_m$ = set of m users that have to be served, R_t = total throughput target for UEs, n_{RB} = number of resource blocks,

TABLE 6. Traffic steering resource block allocation algorithm.

Initialize: $n_{RB}, \chi_{i,j}, \chi_{th}, \forall_j \in U, \forall_j \in N$
Set n_{RB}=0, $\forall_j \in U$
for $k = 1 : T$
  for $i = 1 : N$
    if $\chi_{i,j} < \chi_{th}$ then
      Position of $U = \chi_{i,j}$, n_{RB} are updated
      for $j = 1 : U$
        Compute $\rho_j = \sum_{i \in N} \chi_{i,j} \beta_{i,j} log_2(1 + SINR_{i,j})$
        if $\chi_{i,j} = 1$ && $\rho_j < R_t$ then
          Increment n_{RB}
          $\beta_{i,j} = n_{RB} W_{RB}$
        end if
      end for
      Assigned all RBs or R_t is reached by all active UEs; updated $\chi_{i,j}$
    end if
  end for
end for
if all UEs are satisfied and residual RBs remains than
share equally in candidate space
end if

W_{RB} = BW of a single RB, $\beta_{i,j}$ = bandwidth assigned by BS_i to UE_j. Binary variable $\chi_{i,j}$ signifies the association policy between BSs and UEs, as in the following

$$\chi_{i,j} = \begin{cases} 1, & if \quad UE_j \quad is \quad served \quad by \quad BS_i \\ 0, & otherwise; \forall_i \in N, \forall_j \in U \end{cases}$$

H. LOAD BALANCING CONCEPT

All the nineteen BSs in a two-tier cellular network will be sorted according to their arrival traffic rate, received signal power, and available energy in ascending order. As a consequence, seven cells act as a central BS in a cluster that is surrounded by the neighboring BSs. For instance, a center BS1 is surrounded by the neighboring BS2, BS3, BS4, BS5, and BS6 base stations who are serving as acceptors allowing BS1 to switch into a dormant mode for energy saving according to Fig. 5. Under this scenario, acceptor BSs are adjusting their transmitted power for the extended coverage areas while the donor BS is fully unaware of new traffic arrivals. In the case of high traffic density, the center BS will search the neighboring BSs for sharing the load and a percentage of the load can be transferred to the low traffic density BSs based on the proposed heuristic algorithm. Hence, the neighboring BSs will serve as acceptor BSs by receiving the shifted load and the center BS will act as a donor BS. In the case of very low traffic density, the center BS will shift the load to the neighboring low-density BSs and will go to sleep mode for saving the energy. If the traffic density is high again, the active BSs will send a message to the center BS to wake-up to reduce the load of the neighboring BSs. Notably, this coordination process can be accomplished by a control server by adjusting the coverage area and transmitting the power of the acceptor BSs. In this paper, the idea of network cooperation is governed by the traffic state of the donor BS itself and its acceptor BSs. In a load balancing technique, the adjacent BSs are capable of coordinating each other in a cluster. Employing this dynamic load balancing, energy efficiency performance can be significantly improved through adaptively adjusting the active BSs.

For the traffic distribution, the donor BS selects the best combination of candidate space that can maintain expected QoS. Therefore, different acceptor BSs selection schemes are possible for selecting the best combination of candidate space. Consider a selection scheme C_n, which implies a candidate space containing a set of candidate BS combinations from acceptor BSs (N_a) up to N_s neighbor BSs. Then the selection scheme can be defined as C_n ($N_a \leq N_s$), since the total number of candidate combinations $\sum_{c=1}^{N_a} \binom{N_s}{c}$

For example, if the selection scheme is C_1 for BS1, the candidate space for this donor BS contains the following combinations of BSs: {BS2}, {BS3}, {BS4}, {BS5}, {BS6}, {BS2, BS3}, {BS2, BS4}, {BS2, BS5}, {BS2, BS6}, {BS3, BS4}, {BS3, BS5}, {BS3, BS6}, {BS4, BS5}, {BS4, BS6}, {BS5, BS6}, {BS2, BS3, BS4}, {BS2, BS3, BS5}, {BS2, BS3, BS6}....{BS2, BS3, BS4, BS5, BS6}.

The detailed procedure of the load balancing algorithm is demonstrated in Table 7.

In the load balancing algorithm, $S_{i,j} = S_1, S_2, \ldots S_{Zi}$ = set of BSs in operating mode whose traffic is sharing, $C_{i,j} = C_{i,1}, C_{i,2} \ldots C_{i,Mi}$ = candidate BS. $C^a_{i,j}$ = acceptor candidate BS set, and $Z_{i,j}$ = traffic distribution it owns set of operating BSs. On the other hand, $C^s_{i,j} = \beta_i$ goes to sleep mode only when it can redistribute its traffic to all BSs in $S_{i,j}$, $\chi_{i,j} = \chi_1, \chi_2 \ldots \chi_k$ each BS in active mode, $F_{i,j} = \beta_i$ searches best combination BSs (F_{ij}) in C^a_{ij} or C^s_{ij}.

TABLE 7. Load balancing algorithm.

1: Initialize: $S_{i,j}, \chi_{i,j}, \chi_{th}, P^{i,j}_{TX}, C_{i,j}$
2: **if** β_i active, $S_{i,j} = 1$, $\chi_{i,j} < \chi_{th}$, $Z_{i,j} = 0$, and $C^a_{i,j} \neq \phi$
3: Find $F_{i,j} \in C^a_{i,j}$
4: **else if** β_i active, $S_{i,j} = 1$, $\chi_{i,j} < \chi_{th}$, $Z_{i,j} = 0$, and $C_{i,j} = \phi$
5: Stop searching to neighboring acceptor BSs
6: **else** β_i active, $S_{i,j} \neq \phi$, $\chi_{i,j} < \chi_{th}$, $Z_{i,j} \neq 0$, and $C_{i,j} = \phi$
7: Find $F_{i,j} \in C^s_{i,j}$ such that $\chi_{i,j} \subseteq F_{i,j}$
8: **end if**
9: **if** $F_{i,j} \neq \phi$
10: Set $S_{i,j} = 0$, $P^{i,j}_{TX} = 0$, $\chi_{i,j} = 0$
11: Update $S_{m,n}, P^{m,n}_{TX}, \chi_{m,n}$
12: **end if**

1) NUMBER OF SIMULTANEOUS USERS

In order to determine the number of simultaneous users connected to the LTE base stations, we assume that voice data is 64 kbps for full rate and 32 kbps for half rate. It is also considered that the internet data is 256 kbps and video data is 512 kbps. Moreover, the bandwidth required for each number of resource blocks (RBs) is 180 kHz. The number of simultaneous users of LTE eNodeB is calculated as follows:

VoLTE Packet length with all Header = Codec Bits + RTP Header + UDP Header + IP Header.

In the case of the RoHC enabled system, around 300 bits are required for performing a VoLTE voice call under the air interface [58]. For long term evolution, the smallest unit of radio resources is commonly recognized as a physical resource block (PRB). In LTE, one physical resource block has 12 subcarriers and 14 symbols over a 1-millisecond time length, or $12 \times 14 = 168$ resource elements (REs). Some of the REs are engaged by the control symbols (PDCCH) and pilot symbols (RS), which provide around 120 REs available for data broadcast. LTE downlink modulation provisions diverse modulation coding schemes (MCS) for example QPSK, 16 QAM, and 64 QAM for PDSCH which means that each resource can carry 2bits, 4 bits, or 6 bits per symbol respectively.

If we consider that UE is reporting channel quality indicator (CQI) 15, then eNodeB (i.e., LTE BS) use a 64 QAM modulation scheme and a $948/1024 = 0.926$ effective coding rate is applied, which means that each RE holds $6 \times 0.926 = 5.55$ data bits on average. As a consequence, a single PRB can carry $120 \times 5.55 = 666$ data bits which are equivalent to 2 VoLTE voice samples. But LTE scheduler can't assign less than one PRB per user, so this will count that one PRB is required per VoLTE call. In VoLTE,

no re-transmission is desired and voice data is produced every 20 ms to ensure that about 20 VoLTE calls can share the same set of PRB one after other. The maximum amount of VoLTE call that can be supported is calculated as follows

$$N_{VoLTE} = \frac{N_{PRB}}{N_{PRB}/VoLTE} \times 20 \tag{17}$$

where N_{PRB} is the number of available PRB, and N_{PRB}/VoLTE is the number of PRB per VoLTE call.

III. COST MODELING AND OPTIMIZATION

In this work, different types of costs can be evaluated using the HOMER optimization software under different network conditions aiming to minimize the net present cost. The net present cost (NPC) of the proposed model as a summation of capital cost (CC), replacement cost (RC), net present cost (NPC), operation & maintenance cost (OMC), fuel cost (FC), and salvage value (SV) can be expressed as follows [52]

$$NPC = \frac{TAC}{CRF} = CC + RC + OMC + FC - SV \tag{18}$$

where the total annualized cost (TAC) and capital recovery factor (CRF) is calculated by (19) and (20) respectively [52]

$$TAC = TAC_{CC} + TAC_{RC} + TAC_{OMC} \tag{19}$$

$$CRF = \frac{i(1+i)^N}{(1+i)^N - 1} \tag{20}$$

where N is the lifetime of the project and i is the annual real interest rate. The salvage value of the system can be calculated by [52]

$$SV = rep(\frac{rem}{comp}) \tag{21}$$

where *rep*, *rem*, and *comp* respectively are the replacement cost, remaining lifetime, and lifetime of the component.

For ensuring guaranteed continuity of services, a significant amount of excess electricity is required that can be expressed as follows

$$E_{Excess} = E_{Gen} - E_{BS} - E_l \tag{22}$$

where E_l comprises yearly losses of battery and inverter.

One of the major aims of this work is to minimize energy deficiency through maximum utilization of solar energy in conjunction with energy consumption from the grid which in terms reduces NPC. The objective function of the system can be expressed as [55]

$$\text{minimize } NPC \tag{23a}$$

$$\text{subject to } E_{PV} + E_{EG} > 0 \tag{23b}$$

$$E_{PV} + E_{EG} > E_{BS} \tag{23c}$$

$$E_{PV} + E_{EG} + E_{batt} = E_{BS} + E_l \tag{23d}$$

$$E_{Excess} = E_{PV} + E_{EG} - E_{BS} - E_l \tag{23e}$$

TABLE 8. Key parameters and their specifications for HOMER simulation setup [52], [55].

System Components	Parameters	Value
Resources	Solar intensity	4.59 kWh/m^2/day
	Interest rate	6.75%
Solar PV	Operational lifetime	25 years
	Derating factor	0.9
	System tracking	Dual-axis
	CC	\$1/W
	RC	\$1/W
	OMC/year	\$0.01/W
Electrical Grid	Energy purchase price	\$0.122/kWh
	Energy sellback price	\$0.110/kWh
	Demand charge	\$0.350/kW/month
Battery	Round trip efficiency	85%
	$B_{SoC_{min}}$	30%
	V_{nom}	6 V
	Q_{nom}	360 Ah
	CC	\$300/unit
	RC	\$300/unit
	OMC/year	\$10/unit
Converter	Efficiency	95%
	Operational lifetime	15 years
	CC	\$0.4/W
	RC	\$0.4/W
	OMC/year	\$0.01/W

where E_{BS} is the annual BS load consumption as obtained from Table 3 and E_{batt} is the energy afforded by the battery bank.

The constraint (23b) and (23c) guarantees that the energy generated by the grid-connected solar PV system carries the annual BS consumption. The constraint (23d) represents that the total generated energy including battery backup can satisfy the BS total energy demand and associated losses of the BSs. After fulfilling the energy demand of the BSs, a minimum of 10% of the additional energy is stored in the battery bank (excess electricity) for use in the critical condition and the other 90% energy is allowed for sharing which is represented in constraint (23e).

IV. PERFORMANCE ANALYSIS

A. SIMULATION SETUP

In this simulation setup, the considered project duration is 20 years and the yearly interest rate is 6.75%. The average yearly solar radiation of the selected location is 4.59 $kWh/m^2/day$. Fig. 2 demonstrates the average yearly solar intensity profile of the selected area. The dual-axis tracking mode of the solar PV panels is designed and 10% back power is reserved to support the BS load in any critical condition. However, HOMER optimization software takes decides at each time slot to fulfill the BS energy demand at the lower NPC, according to the predefined constraint. The key component and their technical specifications for the HOMER simulation setup are shown in Table 8. Moreover, the key parameters and their specifications for the Monte-Caro simulation setup are presented in Table 4. The technical parameters that are related to the cell zooming option are

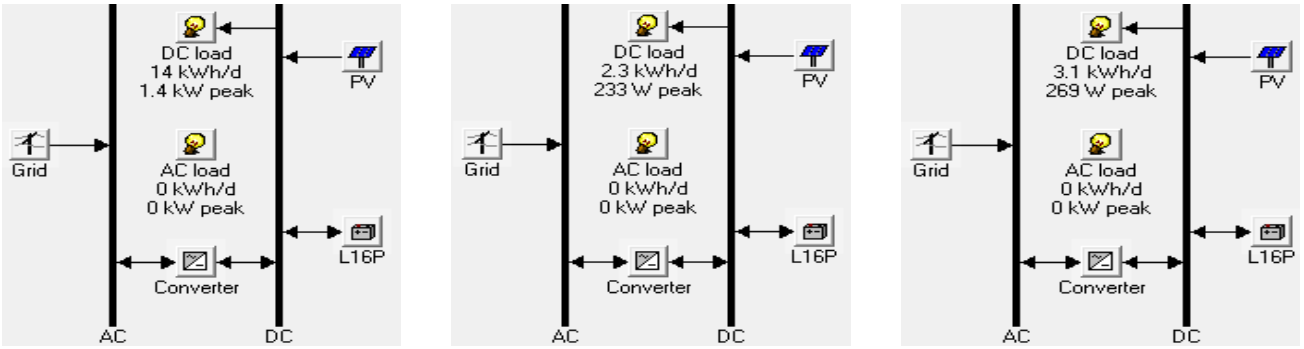

(a) Macro 2/2/2 (b) Macro Omni (c) Micro

FIGURE 7. Schematic diagram of the proposed system in the HOMER platform.

TABLE 9. Zooming options for Macrocell [56].

Radius	400 m	600 m	800 m	1000 m
Power radiated	17 W	25 W	33 W	40 W
Zooming level	40%	60%	80%	100%

TABLE 10. Zooming options for Microcell [56].

Radius	50 m	100 m	200 m	400 m	500 m
Power radiated	5 mW	210 mW	4.1 W	8.4W	10.25 W
Zooming level	20%	50%	100%	200%	250%

summarized in Table 9 and Table 10 respectively for macro and micro BS.

B. OPTIMAL SYSTEM ARCHITECTURE

The HOMER layout of the proposed system for different base station configurations are shown in Fig. 7(a), (b) and (c) under 10 MHz bandwidth. As refer to Table 1, a greater amount of DC load is found for the macro 2/2/2 configuration to support the six transceiver antenna. The optimal system architecture of the macro 2/2/2, macro omni, and micro configurations considering the average solar radiation (4.59 $kWh/m^2/day$) is summarized in Table 11. Moreover, Table 12 compares the optimum system architecture for the various solar intensity of the selected location. In line with our expectation, the macro 2/2/2 configuration required higher solar PV panel capacity to satisfy the higher energy demand. It is also found that the capacity of the solar PV panel decreases with the increment of solar intensity. This is happening because the lower capacity of the solar PV panel can produce higher energy during the higher solar intensity time. On the other hand, the optimal size of the electrical grid, battery, and converter remains constant for all BS configurations which imply that the grid tide solar PV system can be implemented easily for different network configurations without changing the size of the components.

The amount of power contributed by the solar PV panel and electrical grid systems under 10 MHz bandwidth is shown in Fig. 8, Fig. 9 and Fig. 10 respectively for the macro 2/2/2, macro omni, and micro enabled base station systems.

TABLE 11. Optimal system architecture under 10MHz bandwidth.

Components	Optimal Size		
	Macro 2/2/2	Macro Omni	Micro
Solar PV (kW)	3	1	1
Electrical Grid (kW)	10	20	20
Battery (Units)	20	20	20
Converter (kW)	0.1	0.1	0.1

As is seen, the solar PV panel generates a greater amount of renewable energy for all conditions due to the higher value of sunlight intensity in the selected location. On the other hand, the electrical grid system contributes the additional energy due to the deficiency of solar energy. The solar PV panel and electrical grid system complement each other. In the case of higher solar intensity, solar PV panel contributes higher energy. Moreover, the backup power is provided by the battery bank in the case of energy shortage by the solar PV and electrical grid system.

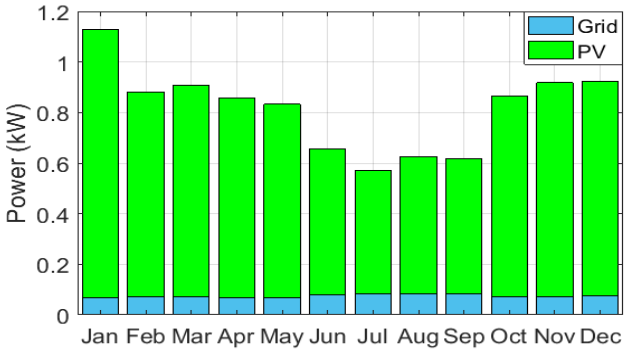

FIGURE 8. Monthly power contribution for Macro 2/2/2 configuration under BW = 10 MHz.

C. ENERGY YIELD ANALYSIS

1) SOLAR PV ENERGY

The optimal size of the solar PV panel to meet the BSs load requirement is presented in Table 11 and 12. As refer to Table 11, the optimal size of the solar PV panel for 10 MHz macro 2/2/2 configuration is 3 kW. Thus, 12 Sharp ND-250QCs solar modules are required for LTE macro

TABLE 12. Summary of technical criteria for the proposed under different solar intensity.

Radiation $(kWh/m2/day)$	PV (kW)			Grid (kW)			Battery (Units)		
	Macro 2/2/2	Macro Omni	Micro	Macro 2/2/2	Macro Omni	Micro	Macro 2/2/2	Macro Omni	Micro
4	2.5	1	1	20	20	20	64	64	64
4.5	3	1	1	20	20	20	64	64	64
5	2.5	1	1	20	20	20	64	64	64
5.5	2.5	1	1	20	20	20	64	64	64

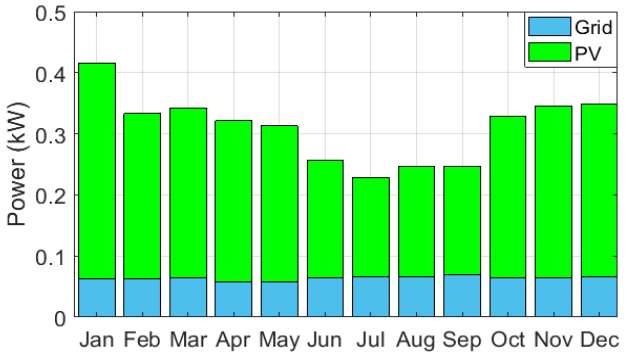

FIGURE 9. Monthly power contribution for Macro omni configuration under BW = 10 MHz.

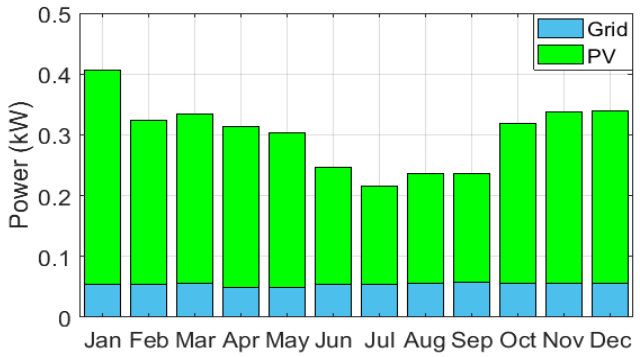

FIGURE 10. Monthly power contribution for Micro configuration under BW = 10 MHz.

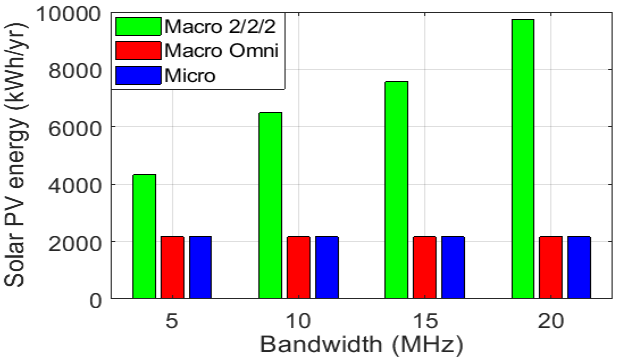

FIGURE 11. Solar energy generation for average solar radiation.

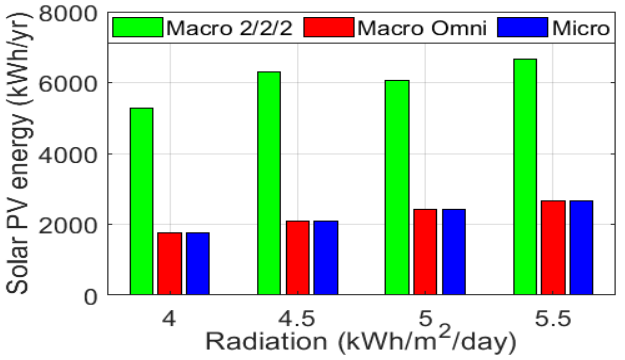

FIGURE 12. Solar energy generation for different solar intensity.

2/2/2 BS configuration: as connected 4 in series and 3 in parallel. The amount of energy harvested by the solar PV panels is calculated using (1) as follows: 3 $kW \times 4.59 \times 0.90 \times 365$ days/year = 4,523 kWh. Moreover, a dual-axis tracker boosts the energy by one fourth which is 6,486 kWh. In a similar process, the annual energy generated and required number of solar PV modules are calculated for other configurations.

On the other hand, the annual energy generated by the solar PV panel for different BSs conditions is shown in Fig. 11 and Fig. 12. According to Table 1, the macro 2/2/2 BS required a higher amount of energy as compared to macro omni and micro BS. As a consequence, the annual energy generated by the solar PV panel is comparatively higher for macro 2/2/2 configuration. It is also noticed that the amount of energy generated by the solar PV panel is rising linearly with the increment of system bandwidth to meet the higher load requirement of the BS.

2) GRID ENERGY

The amount of energy contributed by the electrical grid system is shown in Fig. 13. All the curves are increasing in nature which implies that a higher value of system BW involves a higher amount of grid energy consumption. Moreover, macro 2/2/2 base stations consumed more grid energy as compared to the others because of the higher amount of energy demand.

3) EXCESS ELECTRICITY

The annual energy breakdown for the grid-connected solar PV system is illustrated in Fig. 14. It is always desirable to develop a system that produces a greater amount of renewable energy by utilizing locally available renewable energy sources. In line with our expectations, the solar PV panel generates a significant amount of energy for all network configurations. On the other hand, the electrical grid system contributes a small amount of backup power for ensuring the continuity of power supply. HOMER optimization software

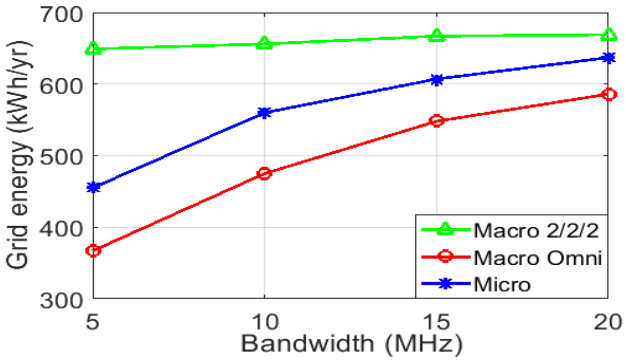

FIGURE 13. Grid energy consumption for different system bandwidth.

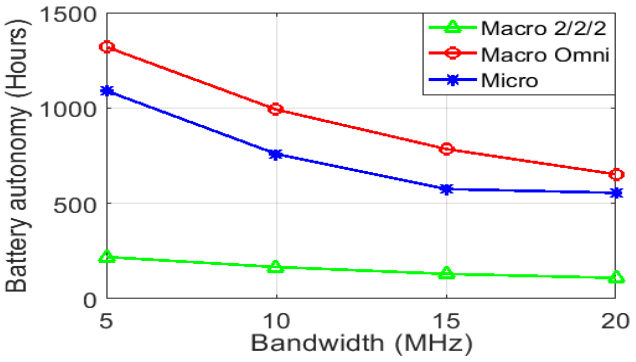

FIGURE 15. Battery bank autonomy for different network configurations.

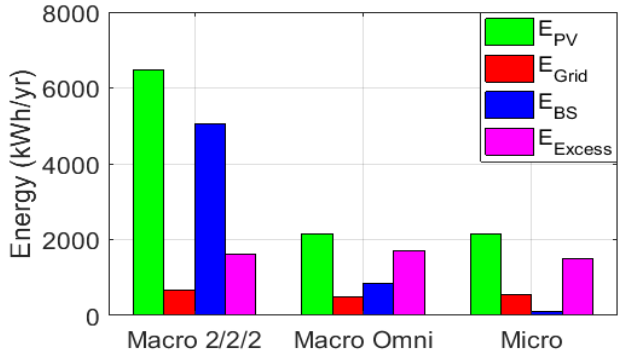

FIGURE 14. Energy breakdown for different network configurations.

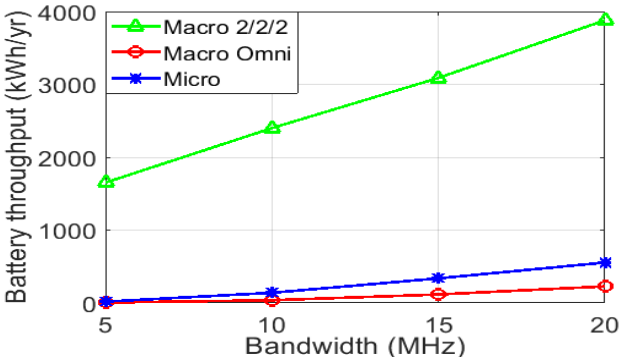

FIGURE 16. Battery bank throughput for different network configurations.

calculates the total amount of energy contributed by the different types of sources and decides at each step to meet the base station energy demand with maximum utilization of renewable energy. However, the total yearly BS energy consumption is 5,042 kWh and the battery and inverter losses are 376 kWh/year and 98 kWh/year respectively. Thus, the yearly excess electricity for 10 MHz bandwidth can be estimated using (22) as follows: (E_{PV}) 6,486 kWh + (E_{EG}) 656 kWh - (E_{BS}) 5,042 kWh- (E_l) 474 kWh = 1,619 kWh/year (32.02%). These values are evaluated for LTE macro 2/2/2 BS considering real traffic patterns and average solar intensity. Similarly, the annual energy generated for all other BSs is calculated.

4) BATTERY BANK

The required number of battery units for macro 2/2/2 BS is 64: 8 batteries connected in series and 8 batteries in parallel. Total time that the battery bank can independently support the BS is 166 hours, which can be found from (3); (64 batteries $\times V_{nom} = 6\ V \times Q_{nom} = 360$ Ah $\times B_{DOD} = 0.7 \times 24$h)/daily average BS load 13.91 kWh. Furthermore, the nominal lifetime of the battery bank is 10 years calculated by (4) for the annual throughput and lifetime throughput of 2,400 kWh and 68,800 kWh respectively. Likewise, HOMER calculates the battery bank autonomy to be 759 hours, battery losses to be 22 kWh/year and the normal battery life is 10 years when the micro configuration is used.

An extensive comparison of battery bank autonomy and throughput for the different network configurations are presented in Fig. 15 and Fig. 16 respectively. As is seen, the battery bank autonomy is inversely proportional to the system bandwidth. However, battery autonomy is more than enough to fix the PV malfunctions or any other failures. On the other hand, the battery bank throughput is directly proportional to the system bandwidth. A higher amount of battery bank throughput is found for macro 2/2/2 configuration.

D. ECONOMIC ANALYSIS

For evaluating the economic feasibility, different types of cost that are associated with the grid-tied solar PV system such as capital cost (CC), operation and maintenance cost (OMC), replacement cost (RC), fuel cost (FC), and the salvage value (SV) incurred within the project lifetime are determined using data from Table 8.

The nominal cash flow summary of the grid-tied solar PV system for the macro 2/2/2, macro omni, and micro configurations are respectively demonstrated in Fig. 17, Fig. 18, and Fig. 19 under 10 MHz bandwidth. For all the configurations, the initial capital cost has the highest value and replacement cost is the second. It is also seen that among the different types of components battery banks incur a large capital cost, replacement cost, O&M cost, and net present cost due to the involvement of a large number of battery units for providing sufficient backup power.

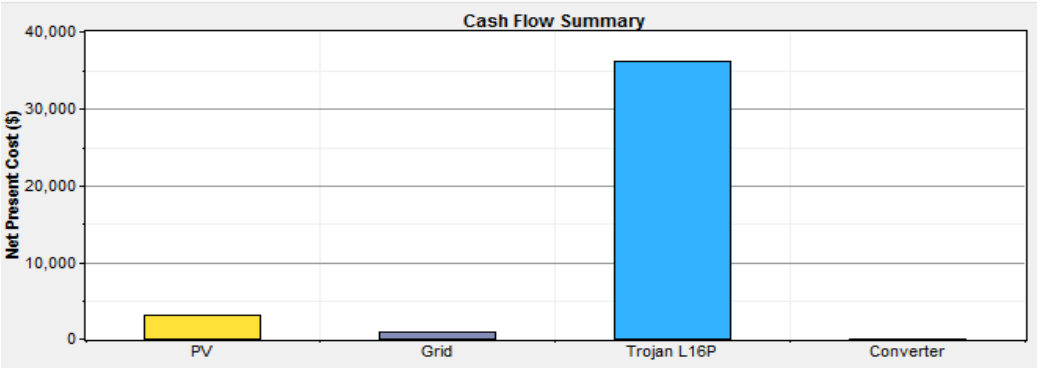

Component	Capital ($)	Replacement ($)	O&M ($)	Fuel ($)	Salvage ($)	Total ($)
PV	3,000	0	324	0	-162	3,162
Grid	0	0	870	0	0	870
Trojan L16P	19,200	9,991	6,914	0	0	36,105
Converter	40	15	11	0	-7	59
System	22,240	10,006	8,119	0	-170	40,195

FIGURE 17. Cash flow summary of the proposed system for Macro 2/2/2 configuration.

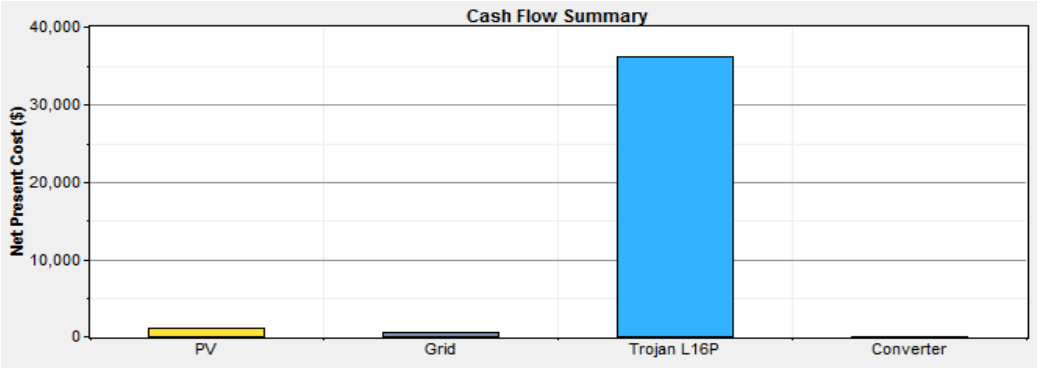

Component	Capital ($)	Replacement ($)	O&M ($)	Fuel ($)	Salvage ($)	Total ($)
PV	1,000	0	108	0	-54	1,054
Grid	0	0	632	0	0	632
Trojan L16P	19,200	9,991	6,914	0	0	36,105
Converter	40	15	11	0	-7	59
System	20,240	10,006	7,665	0	-61	37,850

FIGURE 18. Cash flow summary of the proposed system for Macro omni configuration.

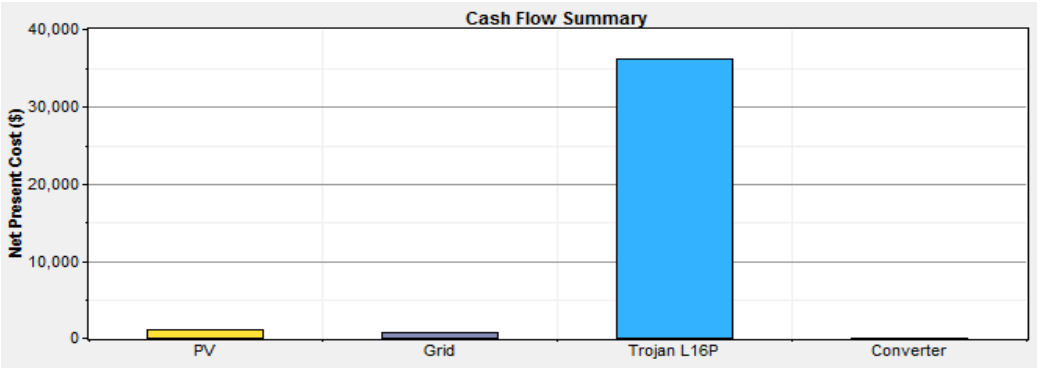

Component	Capital ($)	Replacement ($)	O&M ($)	Fuel ($)	Salvage ($)	Total ($)
PV	1,000	0	108	0	-54	1,054
Grid	0	0	743	0	0	743
Trojan L16P	19,200	9,991	6,914	0	0	36,105
Converter	40	15	11	0	-7	59
System	20,240	10,006	7,776	0	-61	37,961

FIGURE 19. Cash flow summary of the proposed system for Micro configuration.

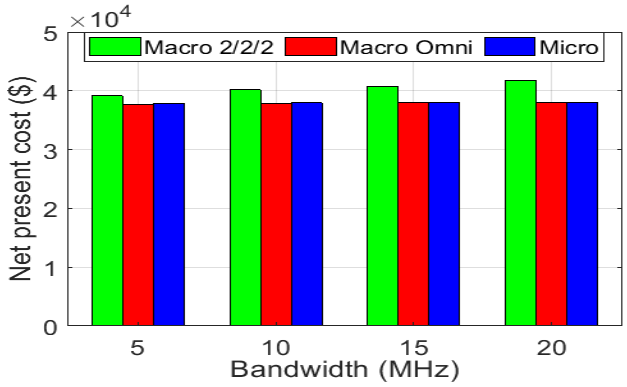

FIGURE 20. NPC of the proposed system.

Fig. 20 represents the quantitative comparison of NPC taking into account the effect of the system bandwidth. The net present cost for the macro 2/2/2, macro omni, and micro BSs under 10 MHz bandwidth are \$40,195, \$37,850, and \$37,961 respectively calculated using (18). In line with our expectations, all the configurations provide a satisfactory level of NPC value. Moreover, the macro 2/2/2 configuration has a higher NPC value due to the higher volume of load demand.

An extensive comparison of the cost of electricity for the aforementioned configuration is demonstrated in Fig. 21. It is found that higher system BW has a positive impact on the curves of electricity cost. It is also found that macro 2/2/2 configuration has the lowest value of COE, whereas macro omni configuration has the highest value. This is happening due to the high volume of energy consumption by the macro 2/2/2 configuration and higher system bandwidth.

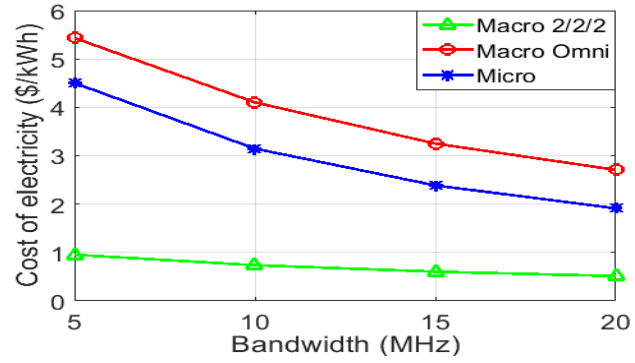

FIGURE 21. COE of the proposed system.

E. CELL ZOOMING AND LOAD BALANCING ANALYSIS

The number of simultaneous users associated with the network under different applications of UEs is presented in Fig. 22. It is seen that among the different types of users, video call users are small in number, and voice call users are large in number. This is happening because the video call required a greater amount of resource block and voice calls required a smaller amount of resource block. A base station can support the higher number of users if the BSs are operated

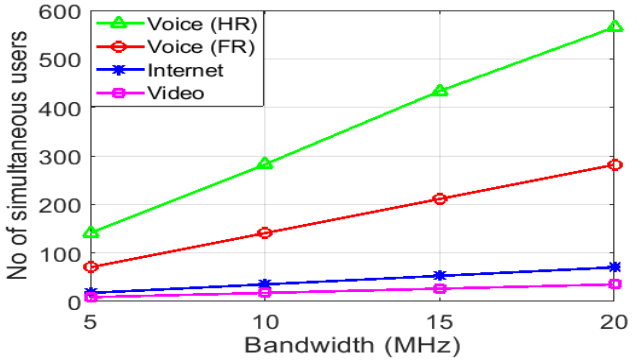

FIGURE 22. The number of simultaneous users under different applications of UEs.

at higher system bandwidth. However, all the users are not connected at the same time and different types of users will go through different applications. As a result, if we consider that 50% voice users, 35% internet users, and 15% of video users are simultaneously connected to the network, we will get the total number of connected users. These values can increase with the increment of system bandwidth as shown in Fig. 23.

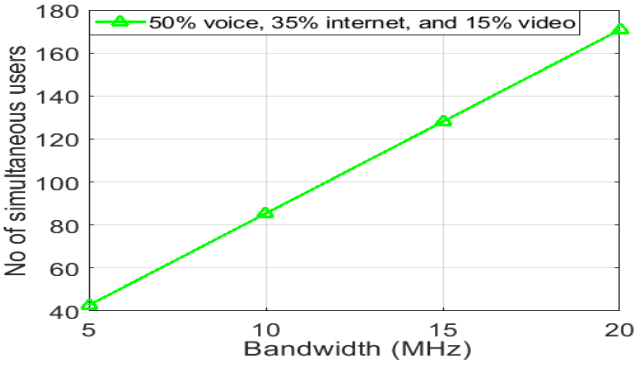

FIGURE 23. The average number of simultaneous users under different applications of UEs.

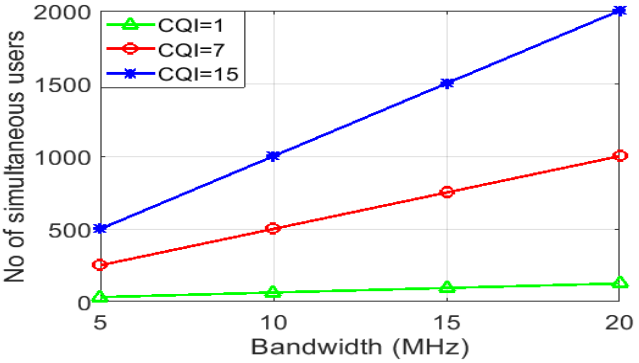

FIGURE 24. The number of simultaneous users for VoLTE under different applications of UEs.

Fig. 24 illustrates the number of simultaneous users for voice over LTE (VoLTE) under different system bandwidth. For VoLTE, the number of simultaneous users depends on the number of resource blocks required, which is directly

related to the modulation technique used which depends on the radio condition of the UE. Different types of modulation schemes can be applied in the LTE system and UE reports RF conditions with channel quality indicator (CQI) to eNodeB and using this report, eNodeB decides the modulation for a particular resource block. The CQI values can be found from 1-15 where 15 provides the best channel condition. Under the best CQI, the best MCS can be used and the number of simultaneous users can be increased. Moreover, continuous improvement of simultaneous users can be obtained for higher system bandwidth for the eNodeB.

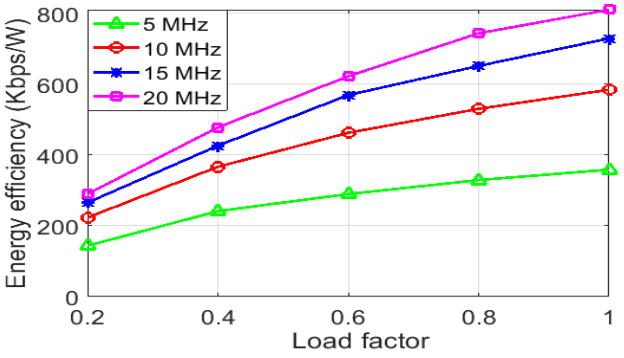

FIGURE 25. The variation of energy efficiency concerning the load factor under different system bandwidth.

The variation of energy efficiency performance concerning the effect of load factor for different system bandwidth is shown in Fig. 25. Where the term 'load factor' is defined as the ratio of maximum load to the actual value of the load in the network. Fig. 25 implies that the BSs operated at lower traffic density, provide lower energy efficiency. On the other, if the BSs are operated at higher traffic density than the average, it will offer relatively higher EE performance. For instance, under 10 MHz bandwidth, when the BSs are operated without applying a load balancing algorithm the energy efficiency becomes 254.4 Kbps/W. In contrast, if the BSs are operated by applying the load balancing algorithm, the EE can vary from 223.37 Kbps/W to 584.48 Kbps/W. Moreover, the load balancing algorithm saves energy by offering the sleep mode provision for the lower density BSs.

The phenomenon of diverse traffic intensity BSs offers that some of the lower density BSs can be switched off or sent to sleep mode by applying the load balancing algorithm. The amount of average energy saved by the sleep mode provision of BS is presented in Fig. 26. In line with our expectation, the energy-saving curves of the BS are increasing linearly with the increment of sleeping hours. Moreover, a higher system bandwidth exhibits a higher amount of energy saving. From the average energy saving curves, it is found that a 4 hours sleeping provision per day can attain 1,100 kWh energy saving annually in the case of 10 MHz bandwidth.

Fig. 27 illustrates that a significant amount of energy and power can be saved by zooming in the cell coverage area. As is seen, the amount of energy saved is linearly and the power consumption is inversely related to the zooming level

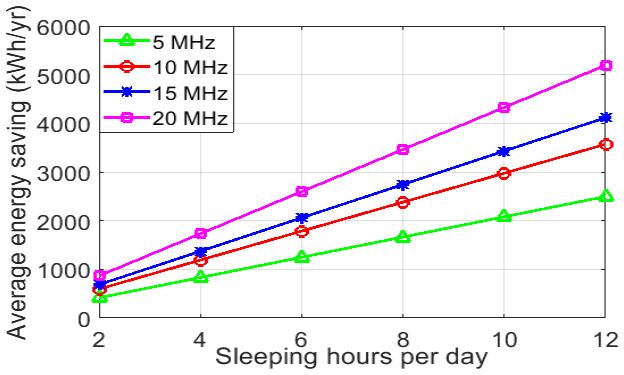

FIGURE 26. Average energy saving vs. sleeping hours of the BS.

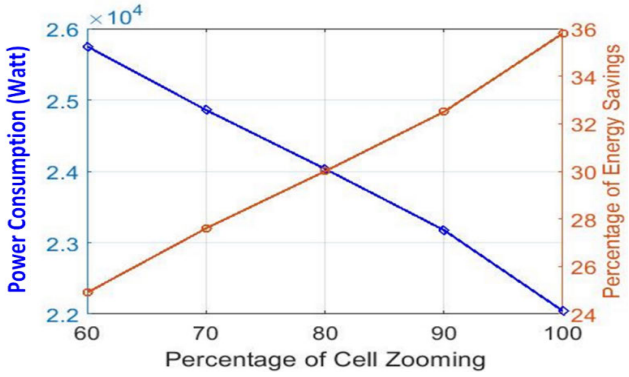

FIGURE 27. Power consumption and percentage of energy saving for different zooming level.

of the cell. For an instance, 80% of cell zooming can save around 30 of the energy requirement. The cell zooming techniques also increase the EE performance of the base station. However, cell zooming is an effective way of developing a smart cellular network but, it is not practicable for the high traffic density areas.

The spectral efficiency of the wireless network can be improved by applying the load balancing algorithm. A detailed comparison of spectral efficiency for the different system bandwidth and different transmission power is shown in Fig. 28. Numerical results depict that the increment of spectral efficiency is directly related to the shifting of load and a 5% edge zone load shifting can increase the spectral efficiency of around 4%.

1) CHALLENGES OF CELL ZOOMING

The cell zooming technique has many potential benefits but the implementation of the cell zooming technique involves some challenges. The major challenges of implementing the cell zooming technique are summarized below:

1. The implementation of the cell zooming technique requires tracing the actual traffic intensity profile and sharing the information to the control server (CS).

2. The implementation of the cell zooming technique requires a proper cooperation management system to control the antenna height, antenna tilt, transmitting power, BS cooperation, and relaying techniques.

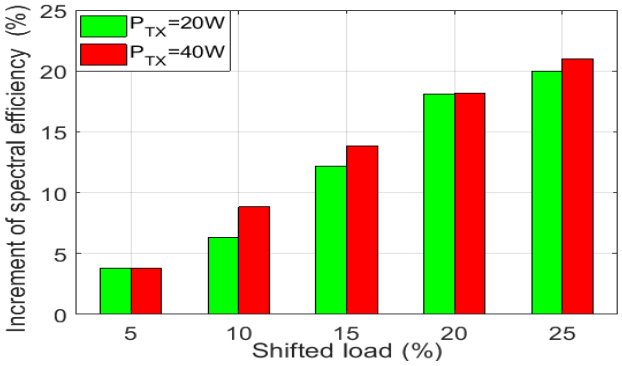

FIGURE 28. Increment of average spectral efficiency vs. percentage of shifted load for macro 2/2/2 configuration.

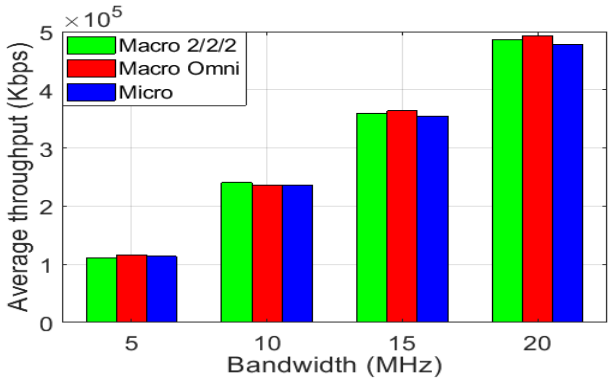

FIGURE 30. Throughput performance for different system bandwidth.

3. The implementation of the cell zooming technique may increase the inter-cell interference and coverage hole. In a BS some users move from one BS to another BS or new users arrive. To satisfy the user demand, some cells need to zoom in and some cells need to zoom out which may cause this inter-cell interference and coverage hole problems.

From the aforementioned discussion, it is concluded that the implementation of the cell zooming scheme is challenging since the sleep and wakeup mechanism are not still considered a mature method. It is not so easy to practically construct an infrastructure due to the aforementioned issues. On the other hand, load balancing is a popular technique that can provide a similar benefit by finding the optimal traffic handover between the overloaded and nearby under loaded cells using the BS coordination mechanism. The key difference between the two mechanisms is that the lightly loaded BS goes to idle mode instead of sleep mode under load balancing concept. Although cell zooming and load balancing techniques exhibit similar performance in terms of energy efficiency, the load balancing technique draws more attention over the cell zooming technique since no sleep mode transition is provisioned.

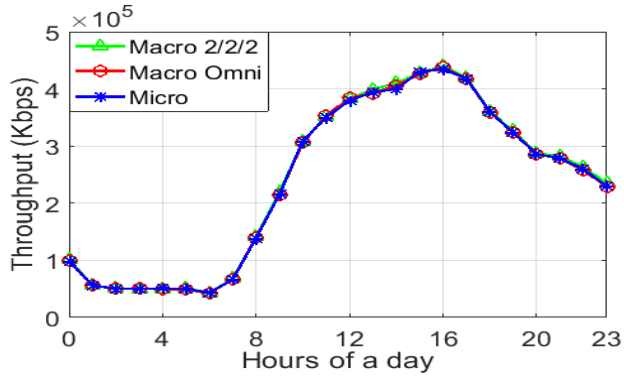

FIGURE 29. Throughput performance over a day.

F. ENERGY EFFICIENCY ANALYSIS

The throughput performance of the proposed system over 24 hours is shown in Fig. 29. The throughput curves for different network configurations follow a similar pattern of traffic demand profile. This is happening because the throughput is directly related to the resource blocks and resource block is a function of traffic demand profile. However, a higher number of RBs are allocated for operating the BS in higher system BW. On the other hand, the throughput performance for different system bandwidth is presented in Fig. 30. It is found that throughput values are increasing linearly with the increment of system bandwidth for all network configurations. Moreover, there is a little difference between the throughput values of macro 2/2/2, macro omni, and micro, but it is not seen clearly due to the high value of throughput. An extensive comparison of energy efficiency performance among the aforementioned network configurations considering the effect of dynamic traffic rate is shown in Fig. 31. The graph tells that the macro omni configuration has superior energy efficiency performance, and the macro 2/2/2 configuration has poor energy efficiency performance. Moreover, higher system bandwidth increases the EE performance of the system under all conditions. All the throughput and energy efficiency have been calculated considering the effect of inter-cell interference (ICI). A higher value of throughput and energy efficiency are always preferable for ensuring the guaranteed quality of services.

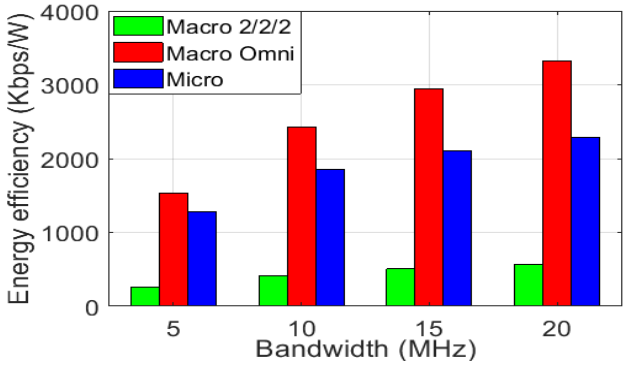

FIGURE 31. Energy efficiency performance for different system bandwidth.

G. CARBON FOOTPRINTS

As an ideal renewable energy source, solar PV system does not emit any carbon content. On the other hand,

TABLE 13. Technical criteria comparison among the different supply scheme under BW = 10 MHz.

Supply scheme	NPC ($)			COE ($)			CO_2 (kg/year)			Excess Electricity (kWh/year)		
	Macro 2/2/2	Macro Omni	Micro	Macro 2/2/2	Macro Omni	Micro	Macro 2/2/2	Macro Omni	Micro	Macro 2/2/2	Macro Omni	Micro
Solar PV/battery	39,852	37,218	37,218	0.733	4.034	3.085	0	0	0	1,064	1,231	940
Grid/battery	44,113	37,918	37,962	0.824	4.101	3.146	3,656	599	829	0.000	0.000	0.000
Solar PV/Grid/battery	40,195	37,850	37,961	0.738	4.102	3.146	415	300	354	1,619	1,706	1,498

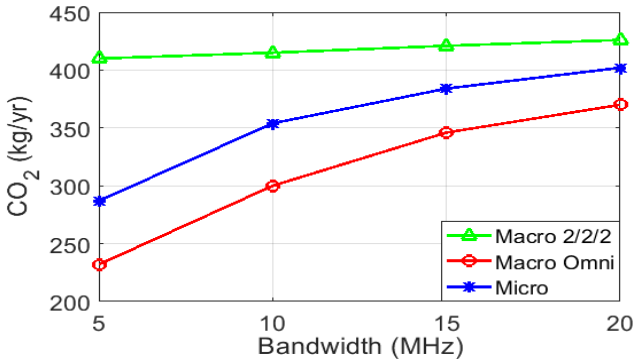

FIGURE 32. Carbon footprints of the proposed system.

a grid-connected solar PV system emits a significant amount of carbon footprints due to the burning of a huge amount of fossil fuel in grid energy generation. Fig. 32 depicts the comparison of carbon footprints generated by a grid-connected solar PV system under different network configurations. The figure illustrates that the macro 2/2/2 configurations produce a greater amount of CO_2. Moreover, higher system BW contributes higher carbon footprints to cope up with the higher BS energy demand. This is happening because a significant amount of energy contribution takes place by the electrical grid system to maintain the continuity of the power supply.

H. FEASIBILITY COMPARISON

A detailed comparison of optimal criteria among the stand-alone solar PV, stand-alone grid, and grid-connected solar PV system along with sufficiency energy storage devices is shown in Table 13. It is found that the grid-connected solar PV system under macro 2/2/2 configuration can attain NPC and COE saving up to 8.8% and 10.43% respectively as compared to the stand-alone grid system. Moreover, it can save carbon footprints by around 88.64%.

V. CONCLUSION

This paper examined the feasibility of macro 2/2/2, macro omni, and micro BS provisioned to be powered by the grid-connected solar PV system with sufficient storage devices. The optimal system criteria including the technical and economic performance of the proposed system have been extensively evaluated under different system bandwidth. The numerical results depict that the grid-tied solar PV system with macro 2/2/2 configuration significantly saves 8.8% of the overall net present cost and achieves a substantial improvement in CO_2 savings yielding up to 88.64%. The battery bank can supply the macro 2/2/2 BS for 166 hours autonomously if the solar PV/grid system fails to support the BS energy demand. On the other hand, the wireless network exhibits a satisfactory level of throughput, energy efficiency, and spectral efficiency performance. Moreover, the incorporation of load balancing techniques can increase the energy efficiency performance up to 56.47% if BSs are effectively modeled with cooperation mechanisms. The load coordination technique gives better utilization of resources in case of average spectral efficiency over cell zooming condition and thereby makes the system more lucrative. In summary, the solar PV/grid-powered heterogeneous cellular network along with the load balancing technique is an excellent choice for developing an energy-efficient and sustainable green mobile communication which will minimize the grid pressure, carbon footprints, and net present cost. In future work, the authors will focus on a coordinated multipoint (CoMP) technique based user association algorithm for multi-tier networks considering a generalized stochastic geometry-based model.

REFERENCES

[1] P. Jonsson, S. Carson, J. S. Sethi, M. Arvedson, R. Svenningsson, P. Lindberg, and K. Ohman, "Ericsson mobility report," in *Proc. Ericsson*, Nov. 2017, pp. 1–8.
[2] *World Energy Outlook 2018*. Accessed: Aug. 20, 2020. [Online]. Available: https://www.iea.org/weo2018/
[3] A. Aris and B. Shabani, "Sustainable power supply solutions for off-grid base stations," *Energies*, vol. 8, no. 10, pp. 10904–10941, Sep. 2015.
[4] M. S. Hossain, A. Jahid, K. Ziaul Islam, M. H. Alsharif, and M. F. Rahman, "Multi-objective optimum design of hybrid renewable energy system for sustainable energy supply to a green cellular networks," *Sustainability*, vol. 12, no. 9, p. 3536, Apr. 2020.
[5] V. Chamola and B. Sikdar, "Solar powered cellular base stations: Current scenario, issues and proposed solutions," *IEEE Commun. Mag.*, vol. 54, no. 5, pp. 108–114, May 2016.
[6] M. Ismail, W. Zhuang, E. Serpedin, and K. Qaraqe, "A survey on green mobile networking: From the perspectives of network operators and mobile users," *IEEE Commun. Surveys Tuts.*, vol. 17, no. 3, pp. 1535–1556, 3rd Quart., 2015.
[7] A. Jahid, K. H. Monju, S. Hossain, and F. Hossain, "Hybrid power supply solutions for off-grid green wireless networks," *Int. J. Green Energy*, vol. 16, no. 1, pp. 12–33, Jan. 2019.
[8] A. Jahid and S. Hossain, "Dimensioning of zero grid electricity cellular networking with solar powered off-grid BS," in *Proc. 2nd Int. Conf. Electr. Electron. Eng. (ICEEE)*, Dec. 2017.
[9] T. Han and N. Ansari, "Powering mobile networks with green energy," *IEEE Wireless Commun.*, vol. 21, no. 1, p. 9096, Feb. 2014.
[10] Huawei. *Mobile Networks Go Green*. Accessed: Aug. 20, 2020. [Online]. Available: http://www.huawei.com/en/abouthuawei/publications/communicaite/hw-082734.htm
[11] A. Jahid and S. Hossain, "Intelligent energy cooperation framework for green cellular base stations," in *Proc. Int. Conf. Comput., Commun., Chem., Mater. Electron. Eng. (IC4ME2)*, Rajshahi, Bangladesh, Feb. 2018, pp. 1–6.
[12] M. S. Hossain, A. Jahid, K. Z. Islam, and M. F. Rahman, "Solar PV and biomass resources-based sustainable energy supply for off-grid cellular base stations," *IEEE Access*, vol. 8, pp. 53817–53840, Mar. 2020.

[13] M. H. Alsharif, R. Nordin, N. F. Abdullah, and A. H. Kelechi, "How to make key 5G wireless technologies environmental friendly: A review," *Trans. Emerg. Telecommun. Technol.*, vol. 29, no. 1, pp. 1–32, Nov. 2017.

[14] A. Jahid, A. B. Shams, and M. F. Hossain, "PV-powered CoMP-based green cellular networks with a standby grid supply," *Int. J. Photoenergy*, vol. 2017, Apr. 2017, Art. no. 6189468.

[15] S. Hossain, B. Kumar Raha, D. Paul, and E. Haque, "Optimization and generation of electrical energy using wind flow in rural area of bangladesh," *Res. J. Appl. Sci., Eng. Technol.*, vol. 10, no. 8, pp. 895–902, Jul. 2015.

[16] M. F. Hossain, A. U. Mahin, T. Debnath, F. B. Mosharrof, and K. Z. Islam, "Recent research in cloud radio access network (C-RAN) for 5G cellular systems–A survey," *J. Netw. Comput. Appl.*, vol. 139, pp. 31–48, Aug. 2019.

[17] M. S. Hossain and M. F. Rahman, "Hybrid solar PV/Biomass powered energy efficient remote cellular base stations," *Int. J. Renew. Energy Res.*, vol. 10, no. 1, p. 329–342, Mar. 2020.

[18] A. Jahid, A. B. Shams, and M. F. Hossain, "Energy cooperation among BS with hybrid power supply for DPS CoMP based cellular networks," in *Proc. 2nd Int. Conf. Electr., Comput. Telecommun. Eng. (ICECTE)*, Rajshahi, Bangladesh, Dec. 2016, pp. 1–4.

[19] Q. Liu, T. Han, N. Ansari, and G. Wu, "On designing energy-efficient heterogeneous cloud radio access networks," *IEEE Trans. Green Commun. Netw.*, vol. 2, no. 3, pp. 721–734, Sep. 2018.

[20] N. A. Chughtai, M. Ali, S. Qaisar, M. Imran, M. Naeem, and F. Qamar, "Energy efficient resource allocation for energy harvesting aided H-CRAN," *IEEE Access*, vol. 6, pp. 43990–44001, 2018.

[21] A. Jahid and M. S. Hossain, "Feasibility analysis of solar powered base stations for sustainable heterogeneous networks," in *Proc. IEEE Region 10 Humanitarian Technol. Conf.*, Dhaka, Bangladesh, Dec. 2017, pp. 686–690.

[22] Y. Jiang, Y. Zou, H. Guo, T. A. Tsiftsis, M. R. Bhatnagar, R. C. de Lamare, and Y.-D. Yao, "Joint power and bandwidth allocation for energy-efficient heterogeneous cellular networks," *IEEE Trans. Commun.*, vol. 67, no. 9, pp. 6168–6178, Sep. 2019.

[23] Y. Li, H. Zhang, J. Wang, B. Cao, Q. Liu, and M. Daneshmand, "Energy-efficient deployment and adaptive sleeping in heterogeneous cellular networks," *IEEE Access*, vol. 7, pp. 35838–35850, 2019.

[24] P. Dini, M. Miozzo, N. Bui, and N. Baldo, "A model to analyze the energy savings of base station sleep mode in LTE HetNets," in *Proc. IEEE Int. Conf. Green Comput. Commun.*, Beijing, China, Aug. 2013, pp. 1375–1380.

[25] M. F. Hossain, K. S. Munasinghe, and A. Jamalipour, "Distributed inter-BS cooperation aided energy efficient load balancing for cellular networks," *IEEE Trans. Wireless Commun.*, vol. 12, no. 11, pp. 5929–5939, Nov. 2013.

[26] M. S. Hossain, K. Z. Islam, A. Jahid, K. M. Rahman, S. Ahmed, and M. H. Alsharif, "Renewable energy-aware sustainable cellular networks with load balancing and energy sharing technique," *Sustainability*, to be published.

[27] Q. Ye, B. Rong, Y. Chen, M. Al-Shalash, C. Caramanis, and J. G. Andrews, "User association for load balancing in heterogeneous cellular networks," *IEEE Trans. Wireless Commun.*, vol. 12, no. 6, pp. 2706–2716, Jun. 2013.

[28] I. Siomina and D. Yuan, "Load balancing in heterogeneous LTE: Range optimization via cell offset and load-coupling characterization," in *Proc. IEEE Int. Conf. Commun. (ICC)*, Ottawa, ON, USA, Jun. 2012, pp. 1357–1361.

[29] Q. Fan and N. Ansari, "Towards throughput aware and energy aware traffic load balancing in heterogeneous networks with hybrid power supplies," *IEEE Trans. Green Commun. Netw.*, vol. 2, no. 4, pp. 890–898, Dec. 2018.

[30] L. A. Fletscher, L. A. Suarez, D. Grace, C. V. Peroni, and J. M. Maestre, "Energy-aware resource management in heterogeneous cellular networks with hybrid energy sources," *IEEE Trans. Netw. Service Manage.*, vol. 16, no. 1, pp. 279–293, Mar. 2019.

[31] T. Zhou, Z. Liu, J. Zhao, C. Li, and L. Yang, "Joint user association and power control for load balancing in downlink heterogeneous cellular networks," *IEEE Trans. Veh. Technol.*, vol. 67, no. 3, pp. 2582–2593, Mar. 2018.

[32] M. M. Hasan and S. Kwon, "Cluster-based load balancing algorithm for ultra-dense heterogeneous networks," *IEEE Access*, vol. 8, pp. 2153–2162, 2020.

[33] A. Jahid, K. Z. Islam, M. S. Hossain, M. K. Hasan Monju, and M. F. Rahman, "Performance evaluation of cloud radio access network with hybrid power supplies," in *Proc. Int. Conf. Sustain. Technol. Ind. (STI)*, Dhaka, Bangladesh, Dec. 2019, pp. 1–5.

[34] M. S. Hossain, A. Jahid, and M. F. Rahman, "Dynamic load management framework for off-grid base stations with hybrid power supply," in *Proc. 4th Int. Conf. Electr. Eng. Inf. Commun. Technol. (iCEEiCT)*, Dhaka, Bangladesh, Sep. 2018, pp. 336–341.

[35] E. Oh, B. Krishnamachari, X. Liu, and Z. Niu, "Toward dynamic energyefficient operation of cellular network infrastructure," *IEEE Commun. Mag.*, vol. 49, no. 6, p. 56–61, Jun. 2011.

[36] S. Kyuho, K. Hongseok, Y. Yung, and B. Krishnamachari, "Base station operation and user association mechanisms for energy-delay tradeoffs in green cellular networks," *IEEE J. Sel. Areas Commun.*, vol. 29, no. 8, p. 1525–1536, Sep. 2011.

[37] K. Son, E. Oh, and B. Krishnamachari, "Energy-aware hierarchical cell configuration: From deployment to operation," in *Proc. IEEE Conf. Comput. Commun. Workshops*, Shanghai, China, Apr. 2011, pp. 289–294.

[38] *LTE; Evolved Universal Terrestrial Radio Access Network (E-UTRAN); Self-Configuring and Self-Optimizing Network (SON) Use Cases and Solutions*, document 3GPP TR 36.902, ETSI TR 136 902 V9.2.0, ETSI, Paris, France, Sep. 2010.

[39] Z. Niu, Y. Wu, J. Gong, and Z. Yang, "Cell zooming for cost-efficient green cellular networks," *IEEE Commun. Mag.*, vol. 48, no. 11, pp. 74–79, Nov. 2010.

[40] Z. Hongyuan, D. Huaiyu, and Z. Quan, "Base Station cooperation for multiuser MIMO: Joint transmission and BS selection," in *Proc. Conf. Inf. Sci. Syst.*, Princeton, PA, USA, Mar. 2004, pp. 1–6.

[41] K. Lee, J. Lee, G. Park, and J. Kyun Choi, "QoS and power consumption analysis of cooperative multicast scheme with cell zooming," in *Proc. 18th Asia–Pacific Conf. Commun. (APCC)*, Jeju, Island, Oct. 2012, pp. 238–242.

[42] G. Micallef, P. Mogensen, and H.-O. Scheck, "Cell size breathing and possibilities to introduce cell sleep mode," in *Proc. Eur. Wireless Conf. (EW)*, 2010, pp. 111–115.

[43] M. Nahas, S. Abdul-Nabi, L. Bouchnak, and F. Sabeh, "Reducing energy consumption in cellular networks by adjusting transmitted power of base stations," in *Proc. Symp. Broadband Netw. Fast Internet (RELABIRA)*, Baabda, CA, USA, May 2012, pp. 39–44.

[44] C.-C. Hsu, J. M. Chang, Z.-T. Chou, and Z. Abichar, "Optimizing spectrum-energy efficiency in downlink cellular networks," *IEEE Trans. Mobile Comput.*, vol. 13, no. 9, pp. 2100–2112, Sep. 2014.

[45] S. Mollahasani and E. Onur, "Density-aware, Energy- and spectrum-efficient small cell scheduling," *IEEE Access*, vol. 7, pp. 65852–65869, 2019.

[46] X. Xu, C. Yuan, W. Chen, X. Tao, and Y. Sun, "Adaptive cell zooming and sleeping for green heterogeneous ultradense networks," *IEEE Trans. Veh. Technol.*, vol. 67, no. 2, pp. 1612–1621, Feb. 2018.

[47] A. R. Khamesi and M. Zorzi, "Energy harvesting and cell zooming in $K-$ tier heterogeneous random cellular networks," *IEEE Trans. Green Commun. Netw.*, vol. 2, no. 1, pp. 63–73, Mar. 2018.

[48] H. Jiang, S. Yi, L. Wu, H. Leung, Y. Wang, X. Zhou, Y. Chen, and L. Yang, "Data-driven cell zooming for large-scale mobile networks," *IEEE Trans. Netw. Service Manage.*, vol. 15, no. 1, pp. 156–168, Mar. 2018.

[49] R. Litjens and L. Jorguseski, "Potential of energy-oriented network optimisation: Switching off over-capacity in off-peak hours," in *Proc. 21st Annu. IEEE Int. Symp. Pers., Indoor Mobile Radio Commun.*, Instanbul, Turkey, Sep. 2010, pp. 1660–1664.

[50] S. Hossain, A. Jahid, and F. Rahman, "Quantifying potential of hybrid PV/WT power supplies for off-grid LTE base station," in *Proc. Int. Conf. Comput., Commun., Chem., Mater. Electron. Eng.*, Rajshahi, Bangladesh, Feb. 2018, pp. 1–5.

[51] M. S. Hossain, M. Rahman, M. T. Sarker, M. E. Haque, and A. Jahid, "A smart IoT based system for monitoring and controlling the sub-station equipment," *Internet Things*, vol. 7, Sep. 2019, Art. no. 100085.

[52] M. H. Alsharif, "Techno-economic evaluation of a stand-alone power system based on solar power/batteries for global system for mobile communications base stations," *Energies*, vol. 10, no. 3, pp. 1–20, Mar. 2017.

[53] A. Jahid and M. S. Hossain, "Energy-cost aware hybrid power system for off-grid base stations under green cellular networks," in *Proc. 3rd Int. Conf. Electr. Inf. Commun. Technol. (EICT)*, Khulna, Bangladesh, Dec. 2017, pp. 1–6.

[54] A. Jahid, M. S. Hossain, M. K. H. Monju, M. F. Rahman, and M. F. Hossain, "Techno-economic and energy efficiency analysis of optimal power supply solutions for green cellular base stations," *IEEE Access*, vol. 8, pp. 43776–43795, 2020.

[55] A. Jahid, M. K. H. Monju, M. E. Hossain, and M. F. Hossain, "Renewable energy assisted cost aware sustainable off-grid base stations with energy cooperation," *IEEE Access*, vol. 6, pp. 60900–60920, 2018.

[56] M. Nahas, M. Ghantous, K. Al Haj Ismaiil, and B. Assaf, "For better energy consumption and management in future cellular networks," in *Proc. Int. Conf. Renew. Ene. Devel. Countries*, Beirut, Lebanon, Nov. 2014, pp. 127–132.
[57] A. Jahid, M. S. Islam, M. S. Hossain, M. E. Hossain, M. K. H. Monju, and M. F. Hossain, "Toward energy efficiency aware renewable energy management in green cellular network with joint coordination," *IEEE Access*, vol. 7, pp. 75782–75797, 2019.
[58] *VoLTE Cell Capacity- Calculating Packet Size*. Accessed: Sep. 5, 2020. [Online]. Available: https://D:/M%20Sc%20Thesis/New%20Journal/AJSE/VoLTE%20Cell%20Capacity-%20Calculating%20Packet%20Size,%20PRBs%20and%20No%20of%20Users%20-%20Techplayon.html

MD. SANWAR HOSSAIN (Graduate Student Member, IEEE) received the B.Sc. degree in electrical and electronic engineering (EEE) from the Rajshahi University of Engineering and Technology, Rajshahi, Bangladesh, in 2010. He is currently pursuing the M.Sc. degree in electrical electronic and communication engineering with the Military Institute of Science and Technology (MIST). From 2011 to 2015, he was a Lecturer with the Department of EEE, Bangladesh University of Business and Technology, Dhaka, Bangladesh, where he is currently an Assistant Professor. His research interests include green energy, smart grid, and power system optimization.

ABU JAHID (Graduate Student Member, IEEE) received the bachelor's and M.Sc. degrees in electrical engineering from MIST, Dhaka, Bangladesh. He is currently pursuing the Ph.D. degree with the Department of Electrical and Computer Engineering, University of Ottawa, Canada. From 2010 to 2012, he worked as a BSS Engineer at Huawei Technologies, where he researches radio network planning and optimization. He was an Assistant Professor with the Department of EEE, Bangladesh University of Business and Technology, Dhaka, Bangladesh, from 2016 to 2019. His research interests include green cellular networking, photonic integrated circuit, and microwave photonics. He has been serving as a TPC member and reviewer in many reputed international journals and conferences.

KHONDOKER ZIAUL ISLAM received the B.Sc. and M.Sc. degrees in electrical engineering from the Islamic University of Technology (IUT), Bangladesh. He is currently pursuing the Ph.D. degree with the Bangladesh University of Engineering and Technology (BUET), Dhaka, Bangladesh. He is an Assistant Professor with the Electrical and Electronic Engineering Department, Bangladesh University of Business and Technology (BUBT), Dhaka, Bangladesh. His current research interests include C-RAN, 5G cellular networks, green communication, radio resource management, and radio planning for cellular networks.

MOHAMMED H. ALSHARIF received the B.Eng. degree in electrical engineering (communication and control) from the Islamic University of Gaza, Palestine, in 2008, and the M.Sc.Eng. and Ph.D. degrees in electrical engineering (wireless communication and networking) from the National University of Malaysia, Malaysia, in 2012 and 2015, respectively. He joined Sejong University, South Korea, in 2016, where he is currently an Assistant Professor with the Department of Electrical Engineering. His current research interests include wireless communications and networks, including wireless communications, network information theory, the Internet of Things (IoT), green communication, energy-efficient wireless transmission techniques, wireless power transfer, and wireless energy harvesting.

KHONDOKAR MIZANUR RAHMAN has been working as a Research Fellow and Visiting Lecturer in Environmental Engineering with the School of Engineering and the Built Environment, Birmingham City University, since 2014, and a Lecturer in Biology and Environment at Derby University, since January 2020. He has been involved in the field of agriculture and environmental research since 2004. He worked for the Waste and Energy Research Group (WERG), Brighton, from 2008 to 2012, working in the field of sustainable waste management. Currently working with the AD Algae Project (EU project includes four North West European countries)—new technology is being developed to take excess waste nutrients produced from anaerobic digestion of food and farm waste to cultivate algal biomass for animal feed and other products of value (LCA). His research and teaching knowledge includes agriculture and environmental sciences with a specific focus on the biological elements of environmental engineering, agriculture, ecology, renewable energy, and sustainability.

MD. FAYZUR RAHMAN was born in Thakurgaon, Bangladesh, in 1960. He received the B.Sc. degree in electrical and electronic engineering from the Rajshahi Engineering College, Bangladesh, in 1984, the M.Tech. degree in industrial electronics from S. J. College of Engineering, Mysore, India, in 1992, and the Ph.D. degree in energy and environment electromagnetic from Yeungnam University, South Korea, in 2000. He was a Professor in Electrical and Electronic Engineering with the Rajshahi University of Engineering and Technology (RUET), where he has served as the HOD. He has also served as the Departmental Head for two years in the EEE Department and two years in the ETE Department of Daffodil International University. He is currently a Professor and Chairperson with the EEE Department, Green University of Bangladesh. His current research interests are energy and environment electromagnetic, electronics/machine control, and high voltage discharge applications. He is a Fellow of the Institution of Engineer's (IEB), Bangladesh, and a Life Member of the Bangladesh Electronic Society.

MD. FARHAD HOSSAIN (Member, IEEE) received the B.Sc. and M.Sc. degrees in electrical and electronic engineering from the Bangladesh University of Engineering (EEE) and Technology (BUET), Dhaka, Bangladesh, in 2003 and 2005, respectively, and the Ph.D. degree in electrical and information engineering from the University of Sydney, Australia, in 2014. He currently holds the position of Professor with the Department of EEE. He also works as an Electrical and Electronic Engineering Consultant. He has published over 50 refereed articles in highly prestigious journals and conference proceedings. His research interests include green cellular networks, underwater communications, smart grid communications, sensor networks, network architectures/protocols designs, and so on. He has been serving as a TPC member and reviewer in many international journals and conferences. He was a recipient of the Best Paper Award in three international conferences and the Student Travel Grant in the IEEE Global Communications Conference (GLOBECOM), Anaheim, CA, USA, in 2012.